A quantum statistical mechanics model of a three-dimensional linear rigid rotator in a bath of oscillators: IV - steady state dielectric properties induced by AC and DC field coupling

1999 J. Phys. A: Math. Gen. 32 897

(http://iopscience.iop.org/0305-4470/32/6/005)

J. Phys. A: Math. Gen. **32** (1999) 897–920. Printed in the UK PII: S0305-4470(99)92823-8

A quantum statistical mechanics model of a three-dimensional linear rigid rotator in a bath of oscillators: IV—steady state dielectric properties induced by AC and DC field coupling

J T Titantah† and M N Hounkonnou‡

Unité de Recherche en Physique Théorique, Institut de Mathématiques et de Sciences Physiques, BP: 613 Porto-Novo, Republic of Benin

Received 27 March 1998, in final form 2 September 1998

Abstract. The long time effect of a radio frequency (rf) AC field superimposed on a DC field on the electrical susceptibility and the Kerr optical functions of polarizable fluids in inert solvent is analysed. The results obtained for the classical Brownian limit, valid for dense solvent media, well reproduce classical results published in the literature with excellent precisions in inertia, density and temperature dependences. The low-density limit yields absorption–dispersion lines whose widths and shifts are density, inertia and temperature dependent. While the low density and/or large inertia susceptibility is explicitly written as a continued fraction obtained by solving an infinite hierarchy of differential coupled equations, that of the Kerr effect is given in the form of successive convergents of the solutions of an infinite hierarchy of differential difference triplets. The polarization/AC field phase difference is analysed. The effects of the constant field strength and the AC field frequency on the Kerr function are explored. In this paper (paper IV) the derivation of some quoted equations will intentionally be left out as they exist in paper III (Titantah J T and Hounkonnou M N 1997 *J. Phys. A: Math. Gen.* **30** 6347) of which this work is its logical continuation.

1. Introduction

Over the past years, the problem of dielectric relaxation and Kerr effect has been the subject of intense work both theoretically and experimentally. Special emphasis has been given to the classical analysis of the problem. Most of the results published thus far have not gone beyond explaining the observations on classical systems, though it is well known that under certain physical conditions quantum aspects start to influence the physical properties of some media [1]. Since 1994, we have been developing a new quantum approach for the description of dielectric and electro-optical properties of materials [2–4]. In our descriptions, we have shown that widely published classical results [5–20] are well recovered as limiting cases of our more general quantum theory. This paper pursues this study, extending it to the case of DC and AC field couplings. In recent papers [2–4], we derived a master equation describing the evolution of a system of linear rigid rotators in a bath of non-interacting harmonic oscillators. Due to the fact that experimentally observed spectra are accounted for, strongly, by molecular rotational motions, we consider the rotational degrees of freedom of the rotator by defining an orientation operator $\hat{\boldsymbol{u}} = \hat{\mu}/\mu$, where $\hat{\mu}$ is the rotator permanent dipole moment of magnitude μ. The

† Present address: Département de Physique, Université Libre de Bruxelles, Brussels, Belgium.
‡ To whom correspondence should be addressed.

0305-4470/99/060897+24$19.50

master equation for the statistical orientation probability density operator $\hat{\rho}_S(t)$ associated with the motion of the rotator in interaction with the bath and an external driving field is [2, 3]

$$\frac{\partial \hat{\rho}_S(t)}{\partial t} + \frac{\mathrm{i}}{\hbar}[\hat{H}_S, \hat{\rho}_S(t)] + \hat{K}\hat{\rho}_S(t) = -\frac{\mathrm{i}}{\hbar}[\hat{H}_E, \hat{\rho}_S(t)] \tag{1}$$

where $\hat{H}_S$ is the rotator rotational kinetic energy operator, whose eigenvalues are $E_l = (\hbar^2/2I)l(l+1)$ with $l = 0, 1, 2\ldots$ and $\mathrm{i} = \sqrt{-1}$.

The collision term is written as

$$\hat{K}\hat{\rho}_S(t) = \frac{\zeta}{I}\sum_{l=1}^{\infty} l\{A_l^*\hat{\boldsymbol{u}}\cdot\hat{\boldsymbol{u}}_l^-\hat{\rho}_S(t) - A_l\hat{\boldsymbol{u}}\cdot\hat{\rho}_S(t)\hat{\boldsymbol{u}}_l^+ + B_l\hat{\boldsymbol{u}}\cdot\hat{\boldsymbol{u}}_l^+\hat{\rho}_S(t) - B_l^*\hat{\boldsymbol{u}}\cdot\hat{\rho}_S(t)\hat{\boldsymbol{u}}_l^-$$
$$-A_l^*\hat{\boldsymbol{u}}_l^-\cdot\hat{\rho}_S(t)\hat{\boldsymbol{u}} + A_l\hat{\rho}_S(t)\hat{\boldsymbol{u}}_l^+\cdot\hat{\boldsymbol{u}} + B_l^*\hat{\rho}_S(t)\hat{\boldsymbol{u}}_l^-\cdot\hat{\boldsymbol{u}} - B_l\hat{\boldsymbol{u}}_l^+\hat{\rho}_S(t)\cdot\hat{\boldsymbol{u}}\} \tag{2}$$

where

$$A_l = \frac{\omega_D^2}{\omega_D^2+\omega_l^2}\left[1 + N(\omega_l) + \mathrm{i}\left(\kappa(x_l, x_D) - \frac{\omega_l}{2\omega_D}\right)\right] \tag{3}$$

$$B_l = \frac{\omega_D^2}{\omega_D^2+\omega_l^2}\left[N(\omega_l) + \mathrm{i}\left(\kappa(x_l, x_D) + \frac{\omega_l}{2\omega_D}\right)\right] \tag{4}$$

with

$$\kappa(x_l, x_D) = -\left[\frac{1}{x_D} + 2\sum_{n=1}^{\infty}\frac{x_l^2 - 2\pi x_D n}{(x_l + x_D)(x_l^2 + 4\pi^2 n^2)}\right] \tag{5}$$

and

$$x_D = \beta\hbar\omega_D \qquad x_l = \beta\hbar\omega_l \qquad \beta = 1/(k_B T) \qquad n = 1, 2, 3, \ldots. \tag{6}$$

ω_D is the characteristic Debye frequency, k_B the Boltzmann constant, T the absolute temperature and $N(\omega_l)$ the occupation number of the rotator quantum level l (bosonic). A_l^* and B_l^* are the complex conjugates of A_l and B_l, respectively. ζ is the friction coefficient characterizing the effects of the bath oscillator concentration on the rotator dynamics, and I is the rotator moment of inertia.

We use the spherical harmonic expansion of the unit vector operator $\hat{\boldsymbol{u}}$ as [2, 3]

$$\hat{\boldsymbol{u}}(t) = \sum_{l=1}^{\infty}(\hat{\boldsymbol{u}}_l^+(t) + \hat{\boldsymbol{u}}_l^-(t)) \tag{7}$$

where

$$\hat{u}_{l_x}^+(t) = \tfrac{1}{2}\sum_{m=-l}^{l}|l, m\rangle[\langle l-1, m+1|A(l, m) - \langle l-1, m-1|B(l, m)] \tag{8}$$

$$\hat{u}_{l_y}^+(t) = \frac{1}{2\mathrm{i}}\sum_{m=-l}^{l}|l, m\rangle[\langle l-1, m+1|A(l, m) + \langle l-1, m-1|B(l, m)] \tag{9}$$

$$\hat{u}_{l_z}^+(t) = \sum_{m=-l}^{l}|l, m\rangle\langle l-1, m|C(l, m) \tag{10}$$

and

$$\hat{\boldsymbol{u}}_l^-(t) = (\hat{\boldsymbol{u}}_l^+(t))^\dagger. \tag{11}$$

$$A(l, m) = \sqrt{\frac{(l-m)(l-m-1)}{(2l-1)(2l+1)}} \tag{12}$$

$$B(l,m) = \sqrt{\frac{(l+m)(l+m-1)}{(2l-1)(2l+1)}} \tag{13}$$

$$C(l,m) = \sqrt{\frac{(l-m)(l+m)}{(2l-1)(2l+1)}}. \tag{14}$$

The AC–DC field coupling term is

$$\hat{H}_E(t) = \begin{cases} 0 & \text{if } t \leqslant 0 \\ -\mu(E_c + E_a\cos\omega t)\cos\hat{\beta} - \dfrac{\alpha_\parallel - \alpha_\perp}{2}(E_c + E_a\cos\omega t)^2\cos^2\hat{\beta} - \\ -\dfrac{\alpha_\perp}{2}(E_c + E_a\cos\omega t)^2\hat{I} & \text{if } t > 0. \end{cases} \tag{15}$$

$\alpha_\parallel$ and $\alpha_\perp$ are, respectively, the rotator polarizability tensor components parallel and perpendicular to the molecular principal axis. We have assumed that the electric fields are applied along the z-axis of the laboratory frame. $\hat{\beta}$ is the angle between the applied field and the dipolar axis. With this Hamiltonian, the initial condition corresponds to equilibrium under free rotations, $\hat{\rho}(t=0) = \hat{\rho}_S^{eq} = \exp(-\frac{\hat{H}_S}{k_B T})/Z$ where Z is the one-particle rotator partition function.

In [4], we used the master equation we derived in [2] (which we named 'the HN master equation' in our previous papers) to verify the dielectric properties of a system of polar rotators in interaction with a constant electric field of strength E_c. The effects of inertia and bath concentration were intensively explored. Using the rotational Smoluchowski equation [5], Morita *et al* [6] and Matsumoto *et al* [7] presented studies of this problem but the former laid much interest on the effect of the applied field on the Kerr effect relaxation that results from the sudden application of the DC field. By averaging the Langevin equation, Coffey [8, 9] tackled the problem emphasizing the effects of inertia.

In this paper, we consider the effect of coupling a constant DC field with a radio frequency AC field. In this paper, we adopt the notations of paper III [4] so that we can directly exploit existing results therein. The polarization and the Kerr functions can be calculated using the Hounkonnou–Titantah (HT) quantum relations [4]

$$P(t) = \frac{2\mu}{3}\sum_{l=0}^{\infty}(l+1)\frac{\mathrm{e}^{-\beta E_l}}{Z}\mathrm{Re}\,\sigma_{l,l+1}(t) \tag{16}$$

$$\Phi(t) = \frac{2}{15}\sum_{l=0}^{\infty}\frac{\mathrm{e}^{-\beta E_l}}{Z}\frac{(l+1)}{(2l+3)}\left\{\frac{l(2l+1)}{(2l-1)}\varphi_{l,l}(t) + 3(l+2)\mathrm{Re}\,\eta_{l,l+2}(t)\right\} \tag{17}$$

where Z is the one-particle free rotator canonical partition function and Re denotes the real part. The reduced HT equations for the matrix elements $\sigma_{l,l+1}(t)$, $\varphi_{l,l}(t)$, and $\eta_{l,l+2}(t)$ [4] are:

(i) the reduced HT1;

$$\left(\frac{\partial}{\partial t} - \frac{\mathrm{i}\bar{h}}{I}(l+1)\right)\sigma_{l,l+1}(t)$$
$$+B\left[\left\{(A_l^* l^2 + B_{l+1}(l+1)^2)\frac{1}{2l+1} + (A_{l+1}(l+1)^2 + B_{l+2}^*(l+2)^2)\frac{1}{2l+3}\right\}\right.$$
$$\times\sigma_{l,l+1}(t) - \mathrm{e}^{\beta(E_l - E_{l-1})}\frac{l}{2l+1}[B_l l + (l+1)B_{l+1}^*]\sigma_{l-1,l}(t)(1-\delta_{l0})$$
$$-\mathrm{e}^{-\beta(E_{l+1}-E_l)}\frac{l+2}{2l+3}[A_{l+1}^*(l+1) + A_{l+2}(l+2)]\sigma_{l+1,l+2}(t)$$

$$-\frac{l+1}{(2l+1)(2l+3)}[A^*_{l+1}(l+1)+B^*_{l+1}(+1)]\sigma^*_{l,l+1}(t)\Bigg]$$
$$= -\mathrm{i}\frac{\mu E(t)}{\hbar}(1-\mathrm{e}^{-\beta(E_{l+1}-E_l)}) \tag{18}$$

(ii) the reduced HT2;

$$\frac{\partial}{\partial t}\varphi_{l,l}(t)+2B\mathrm{Re}\left\{\frac{(A_l l^2+B_{l+1}(l+1)^2)}{2l+1}\varphi_{l,l}(t)-A_{l+1}(l+1)\right.$$
$$\times\frac{(l+2)(2l-1)}{(2l+1)^2}\mathrm{e}^{-\beta(E_{l+1}-E_l)}\varphi_{l+1,l+1}(t)$$
$$-B_l l\frac{(l-1)(2l+3)}{(2l+1)^2}\mathrm{e}^{\beta(E_l-E_{l-1})}\varphi_{l-1,l-1}(t)(1-\delta_{l0})$$
$$\left.-3\frac{(B_l l+A_{l+1}(l+1))}{(2l+1)^2}\mathrm{e}^{\beta(E_l-E_{l-1})}\eta_{l-1,l+1}(t)(1-\delta_{l0})\right\}$$
$$=\frac{\mu E(t)}{\hbar}\left(\frac{2l-1}{2l+1}\mathrm{Im}\,\sigma_{l,l+1}(t)-\mathrm{e}^{\beta(E_l-E_{l-1})}\frac{2l+3}{2l+1}\mathrm{Im}\,\sigma_{l-1,l}(t)(1-\delta_{l,0})\right) \tag{19}$$

and

(iii) the reduced HT3;

$$\left[\frac{\partial}{\partial t}-\frac{\mathrm{i}\hbar}{I}(2l+3)\right]\eta_{l,l+2}(t)+B\Bigg[\Bigg\{[A^*_l l^2+B_{l+1}(l+1)^2]$$
$$\times\frac{1}{2l+1}+[A_{l+2}(l+2)^2+B^*_{l+3}(l+3)^2]\frac{1}{2l+5}\Bigg\}\eta_{l,l+2}(t)$$
$$-\frac{l}{2l+1}\mathrm{e}^{\beta(E_l-E_{l-1})}[B^*_l l+B_{l+2}(l+2)]\eta_{l-1,l+1}(t)(1-\delta_{l0})$$
$$-\mathrm{e}^{-\beta(E_{l+1}-E_l)}\frac{l+3}{2l+5}[A^*_{l+1}(l+1)+A_{l+3}(l+3)]\eta_{l+1,l+3}(t)$$
$$-\frac{2}{(2l+1)(2l+5)}[A^*_{l+1}(l+1)+B_{l+2}(+2)]\varphi_{l+1,l+1}(t)\Bigg]$$
$$=\mathrm{i}\frac{\mu E(t)}{\hbar}(\mathrm{e}^{-\beta(E_{l+1}-E_l)}\sigma_{l+1,l+2}(t)-\sigma_{l,l+1}(t))$$
$$-\mathrm{i}\frac{\Delta\alpha E(t)^2}{2\hbar}(1-\mathrm{e}^{-\beta(E_{l+2}-E_l)}) \tag{20}$$

where $B=\zeta/I$. The initial conditions on these matrix elements are

$$\sigma_{l,l+1}(t=0)=\varphi_{l,l}(t=0)=\eta_{l,l+2}(t=0)=0.$$

2. On the electrical susceptibility and the Kerr functions

In this section, the calculations of the electrical susceptibility and the Kerr functions are performed in two different physical limits: (1) the classical Brownian limit and (2) the rotating wave approximation (RWA). In each case, we analyse the long-time effect, that is, we consider very long times compared with the period of collision $\tau=1/B$, the Debye relaxation time $\tau_D=\zeta/(2Ik_BT)$ and the mean thermal angular time $(I/k_BT)^{0.5}$.

2.1. The classical Brownian limit

This limit is characterised by slow moving rotators entering into instantaneous collisions with the bath of fast moving oscillators. Inertial effects are very important for understanding line shapes. With the aid of the Fokker–Planck–Kramer (FPK) equation [29, 30, 10–12], Hounkonnou *et al* [11, 13–15] presented the steady state analysis of the electric polarization and the Kerr optical function in a radio frequency AC field; while their electric susceptibility function was given as a continued fraction, the Kerr function was in the form of exponential integrals. Filippini [16] experimentally measured the Kerr dispersion constant when an AC field superimposed on a unidirectional field is applied to a liquid. Coffey and Paranjape [18], Morita [5], Morita and Watanabe [19], gave theoretical descriptions of these phenomena using pure classical diffusion equations.

2.1.1. The electrical susceptibility. In the classical limit, quantum equations reduce to the classical HT equations for the electrical susceptibility [4]

$$P(\tau) = \frac{\mu}{3} S_0^0(\tau) \tag{21}$$

$$\left(\frac{\mathrm{d}}{\mathrm{d}\tau} + 2j\right) S_j^0(\tau) + 2b_2[(j+1)S_j^1(\tau) - jS_{j-1}^1(\tau)] = 0 \tag{22}$$

and

$$\left(\frac{\mathrm{d}}{\mathrm{d}\tau} + 2j + 1\right) S_j^1(\tau) - b_1[S_j^0(\tau) - S_{j+1}^0(\tau)] = -b_1 \frac{\mu E_a}{k_B T}(r + \cos\omega t)\delta_{j,0} \tag{23}$$

where $\tau = Bt$, $\omega' = \omega/B$ are dimensionless time and frequency, respectively; $r = E_c/E_a$ measures the ratio of the constant field strength to the amplitude of the AC field. $b_1 b_2 = \gamma = Ik_B T/\zeta^2$, where ζ is the coupling coefficient. In the steady state regime, we search for $S_j^m(\tau)$ in the forms:

$$\begin{aligned} S_0^0(\omega', \tau) &= \frac{\mu E_a}{k_B T}[r + S_0^{0'}(\omega')\mathrm{e}^{\mathrm{i}\omega'\tau} + (S_0^{0'}(\omega'))^*\mathrm{e}^{-\mathrm{i}\omega'\tau}] \\ S_j^0(\omega', \tau) &= \frac{\mu E_a}{k_B T} S_j^{0'}(\omega')\mathrm{e}^{\mathrm{i}\omega'\tau} + \text{C.C.} \qquad \text{for} \quad j \neq 0 \\ S_j^1(\omega', \tau) &= \frac{\mu E_a}{k_B T} S_j^{1'}(\omega')\mathrm{e}^{\mathrm{i}\omega'\tau} + \text{C.C.} \qquad \text{for all} \quad j \end{aligned} \tag{24}$$

where C.C. denotes complex conjugate. On substituting these into the hierarchy (22), (23) and solving for $S_0^{0'}(\omega')$, we get

$$S_0^{0'}(\omega') = \cfrac{\gamma}{2\gamma + \mathrm{i}\omega'\left[1 + \mathrm{i}\omega' + \cfrac{2\gamma}{2 + \mathrm{i}\omega' + \cfrac{4\gamma}{3 + \mathrm{i}\omega' + \cfrac{4\gamma}{4 + \mathrm{i}\omega' + \cfrac{6\gamma}{5 + \mathrm{i}\omega' + \cdots}}}}\right]} \tag{25}$$

and using (21), we deduce the polarization

$$P(\omega', \tau) = \frac{\mu^2 E_a}{3k_B T}\left\{\frac{r}{2} + \cfrac{\gamma \mathrm{e}^{\mathrm{i}\omega'\tau}}{2\gamma + \mathrm{i}\omega'\left[1 + \mathrm{i}\omega' + \cfrac{2\gamma}{2 + \mathrm{i}\omega' + \cfrac{4\gamma}{3 + \mathrm{i}\omega' + \cfrac{4\gamma}{4 + \mathrm{i}\omega' + \cdots}}}\right]} + \text{C.C.}\right\}. \tag{26}$$

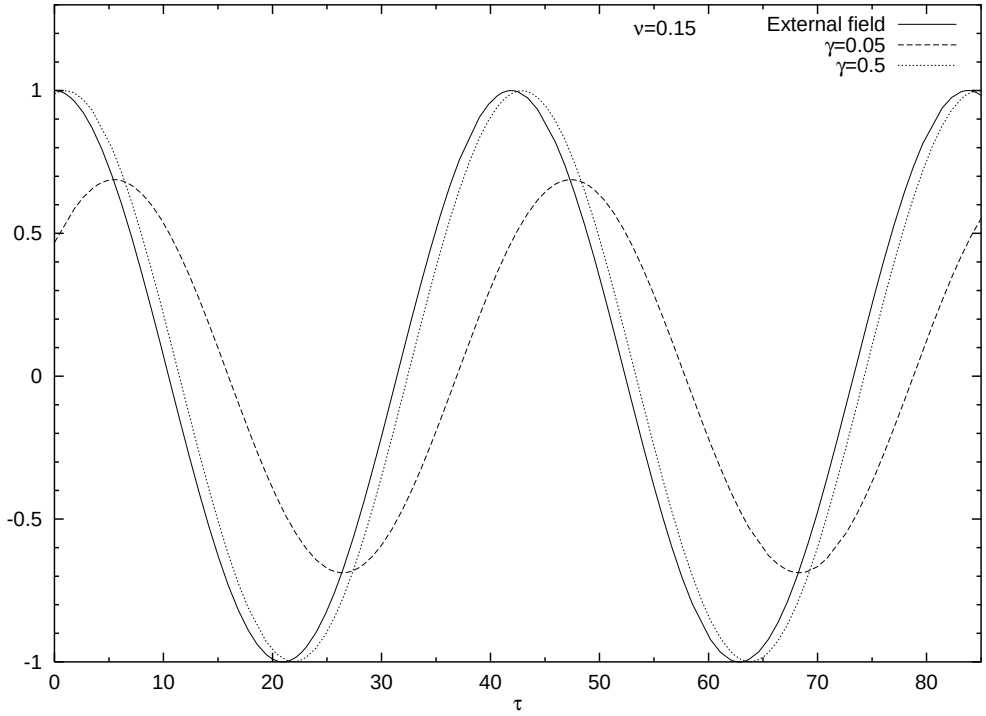

Figure 1. Function $\cos \nu\tau$ (——), the reduced susceptibility $\chi_r(\nu, \tau)$ for the parameter $\gamma = Ik_BT/\zeta^2 = 0.05$ (- - - -) and $\gamma = 0.5$ (·····) against the dimensionless time $\tau = \omega_{mean}t$, provided the fixed reduced frequency $\nu = \omega/\omega_{mean} = 0.15$ and DC field parameter $r = 0$ ($\omega_{mean} = (k_BT/I)^{0.5}$ and $r = E_c^2/(E_c^2 + E_a^2)$).

In the absence of the DC field ($r = 0$), the result of Gross [20] on generalized Brownian motion is recovered. We define a reduced susceptibility $\chi_r(\omega', \tau)$ as

$$\chi_r(\omega', \tau) = r + 2|S_0^{0'}(\omega')| \cos(\omega'\tau - \alpha(\omega')) \tag{27}$$

where $\alpha(\omega,)$, the phase difference between the exciting AC field and the dielectric response function (the polarization), furnishes valuable information on the absorption properties of the medium under investigation. It is given by

$$\tan \alpha(\omega') = -\frac{\text{Im } S_0^{0'}(\omega')}{\text{Re } S_0^{0'}(\omega')}. \tag{28}$$

On neglecting inertial effects in (25), we obtain the Debye limit

$$S_0^{0'}(\omega') = \frac{1}{2(1 + \text{i}\omega\tau_D)} \tag{29}$$

in usual frequency units. In this case, the phase is given by $\tan \alpha(\omega) = \omega\tau_D$ with $\tau_D = \zeta/(2k_BT)$. The lowest inertial limit, corresponding to the Rocard formula,

$$S_0^{0'}(\omega') = \frac{1}{2(1 + \text{i}\omega\tau_D - (I\omega^2/2k_BT))} \tag{30}$$

leads to the phase expression $\tan \alpha(\omega) = \omega\tau_D/(1 - (I\omega^2/2k_BT))$ which yields a maximum phase of $\pi/2$ for frequency of $\sqrt{2}$ times mean thermal agitation frequency ($\omega_{mean} =$

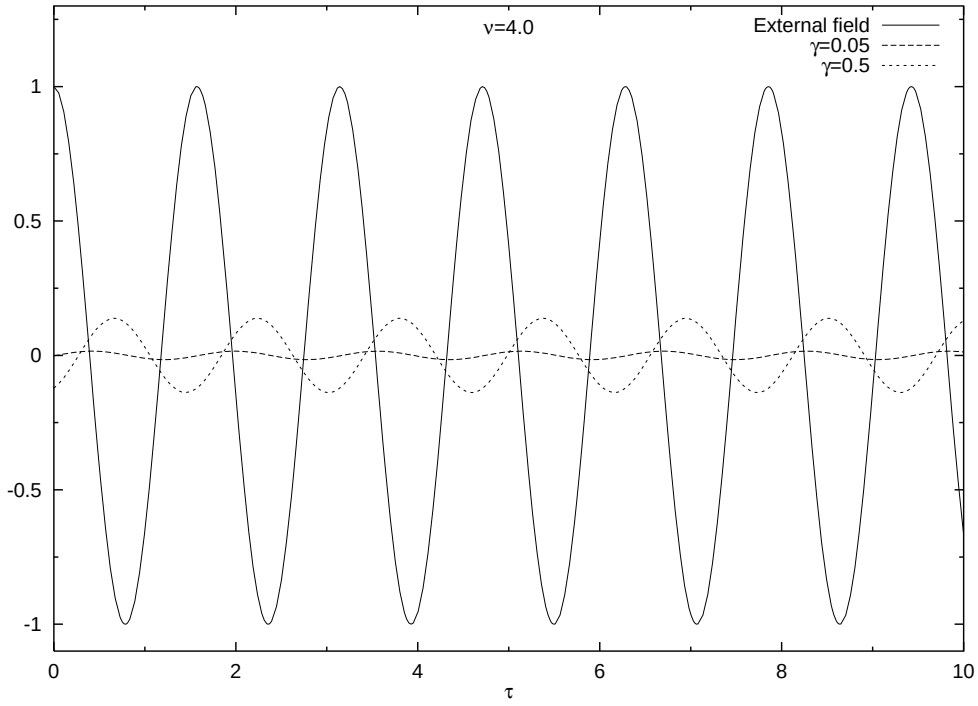

Figure 2. Function $\cos \nu\tau$ (——), the reduced susceptibility $\chi_r(\nu, \tau)$ for the parameter $\gamma = 0.05$ (- - - -) and $\gamma = 0.5$ (· · · · · ·) against the dimensionless time $\tau = \omega_{mean}t$, provided the fixed reduced frequency $\nu = 4.00$ and $r = 0$.

$(k_BT/I)^{0.5}$). At this frequency value, the rate of energy absorption from the surrounding bath by the rotators is in phase with the forcing field (since the rate of heat exchange between the rotator and the surrounding is proportional to minus the rate of change of the induced polarization [3, 4, 17]). On defining a new dimensionless frequency $\nu = \omega/\omega_{mean}$ in (25), we rewrite $S_0^{0'}$ as

$$S_0^{0'}(\nu) = \cfrac{1}{2 + \mathrm{i}\nu/\sqrt{\gamma} - \nu^2 + \cfrac{2\mathrm{i}\sqrt{\gamma}\nu}{2 + \mathrm{i}\sqrt{\gamma}\nu + \cfrac{4\gamma}{3 + \mathrm{i}\sqrt{\gamma}\nu + \cfrac{4\gamma}{4 + \mathrm{i}\sqrt{\gamma}\nu + \cdots}}}}. \qquad (31)$$

Figures 1 and 2 show the plots of the external exciting field $\cos \nu\tau$ and those of the reduced susceptibility $\chi_r(\nu, \tau)$ as functions of the dimensionless time τ (with $\tau = t\omega_{mean}$) for $\nu = 0.15$, 4.00 and for different values of γ. For fixed ω_{mean}, we analyse the effect of friction ζ on the phase, through $\gamma = Ik_BT/\zeta^2$. Figure 3 shows a 3D plot of $\chi_r(\nu, \tau)$ for $\gamma = 0.05$. Figure 4 shows a 3D plot of the tangent of the phase angle as a function of the reduced frequency ν and γ. The peaks are found to shift towards larger frequency values as γ increases. It is important to note that while the Debye theory predicts such phenomena only for infinite frequencies ($\tan \alpha(\omega) = \omega\tau_D$) and the Rocard lowest inertial limit predicts a phase difference of $\pi/2$ between the applied field and the material response at $\nu = \sqrt{2}$, our results extensively portray the effect of inertia on this phase difference. The pioneering investigations of inertial effects in Debye relaxation date back to the work by Sack in 1957 [23] in which he

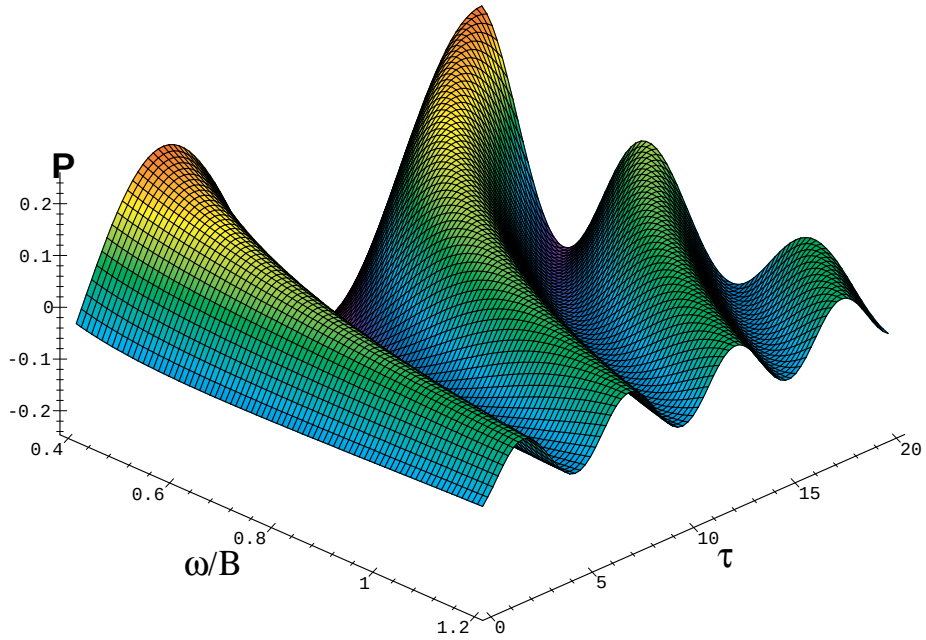

Figure 3. 3D plot of the reduced polarization $\chi_r(\omega', \tau)$ for the inertial parameter $\gamma = 0.05$ and $r = 0$ against the dimensionless time and freqency $\tau = Bt$ ($B = \zeta/I$) and $\omega' = \omega/B$, respectively.

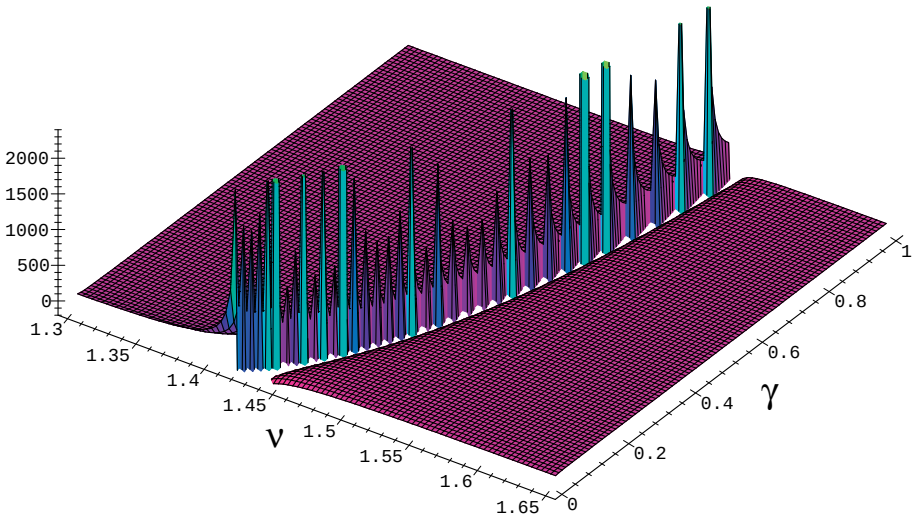

Figure 4. 3D plot of function $\tan\alpha(\nu, \gamma)$ against the dimensionless freqency $\nu = \omega/\omega_{mean}$ and the inertia parameter $\gamma = 0.05$ (classical result).

expressed the dielectric property as a continued fraction.

2.1.2. The Kerr function. The classical HT equations [4] for the optical Kerr function are:

$$\Phi(\tau) = \tfrac{1}{30} Y_0^0(\tau) \tag{32}$$

with

$$\left(\frac{\mathrm{d}}{\mathrm{d}\tau} + 2j\right) Y_j^0(\tau) + 24b_2((j+1)Y_j^1(\tau) - jY_{j-1}^1(\tau))$$
$$= -4b_2 \frac{\mu E_a}{k_B T}(r + \cos\omega'\tau) S_{j-1}^1(\tau)(1 - \delta_{j,0}) \tag{33}$$

$$\left(\frac{\mathrm{d}}{\mathrm{d}\tau} + 2j + 1\right) Y_j^1(\tau) - \frac{b_1}{3}(Y_j^0(\tau) - Y_{j+1}^0(\tau)) + \frac{b_1}{3}(X_j(\tau) - X_{j+1}(\tau))$$
$$= -b_1 \frac{\mu E_a}{k_B T}(r + \cos\omega'\tau) S_j^0(\tau) - b_1 \frac{\Delta\alpha E_a^2}{k_B T}(r + \cos\omega'\tau)^2 \delta_{j,0} \tag{34}$$

$$\left[(2j+1)\left(\frac{\mathrm{d}}{\mathrm{d}\tau} + 2j\right) + 2\right] X_j(\tau) - j\left(\frac{\mathrm{d}}{\mathrm{d}\tau} + 2j - 2\right) X_{j-1}(\tau)$$
$$-(j+1)\left(\frac{\mathrm{d}}{\mathrm{d}\tau} + 2j + 2\right) X_{j+1}(\tau) - \tfrac{1}{2} Y_j^0(\tau)$$
$$= b_2 \frac{\mu E_a}{k_B T}(r + \cos\omega'\tau)[-2j(j-1)S_{j-2}^1(\tau) + j(4j+5)S_{j-1}^1(\tau)$$
$$-(j+1)(2j+3)S_j^1(\tau)]. \tag{35}$$

Steady state solutions are sought in the forms:

$$X_j(\omega', \tau) = \left(\frac{\mu E_a}{k_B T}\right)^2 [X_{j,0}(\omega') + X_{j,1}(\omega')\mathrm{e}^{\mathrm{i}\omega'\tau} + X_{j,2}(\omega')\mathrm{e}^{2\mathrm{i}\omega'\tau} + \text{C.C.}]$$
$$Y_j^0(\omega', \tau) = \left(\frac{\mu E_a}{k_B T}\right)^2 [Y_{j,0}^0(\omega') + Y_{j,1}^0(\omega')\mathrm{e}^{\mathrm{i}\omega'\tau} + Y_{j,2}^0(\omega')\mathrm{e}^{2\mathrm{i}\omega'\tau} + \text{C.C.}] \tag{36}$$
$$Y_j^1(\omega', \tau) = \left(\frac{\mu E_a}{k_B T}\right)^2 [Y_{j,0}^1(\omega') + Y_{j,1}^1(\omega')\mathrm{e}^{\mathrm{i}\omega'\tau} + Y_{j,2}^1(\omega')\mathrm{e}^{2\mathrm{i}\omega'\tau} + \text{C.C.}].$$

Knowing the forms of S_j^m, we obtain the three systems of hierarchies (each system being a set of three coupled equations (triplets)) given in appendix A. The technique adopted in solving these triplets is based on convergents. Note that the systems could be written in matrix forms of infinite dimensions. The notion of convergence can be seen as limiting the dimensions of the matrices. The zeroth convergent consists of considering only equations involving $j = 0$. The first convergent is the modification of the zeroth by including $j = 1$ terms. The former is the solution of a 3×3 matrix equation, while the latter is that of a 6×6 matrix equation. Reliable spectral information can only be obtained from at least a 6×6 matrix equation. The expressions for $Y_{0,0}^0(\omega')$, $Y_{0,1}^0(\omega')$ and $Y_{0,2}^0(\omega')$ obtained for $j = 1$, are given in appendix B, where $R = \mu^2/(\Delta\alpha k_B T)$, $E^2 = E_a^2 + E_c^2$ and $K_0 = (\frac{\mu}{K_B T})^2 + \frac{\Delta\alpha}{K_B T}$. We can now write the Kerr function as

$$\Phi(\omega', \tau) = \tfrac{1}{30} E^2 K_0 [Y_{0,0}^0(\omega') + Y_{0,1}^0(\omega')\exp(\mathrm{i}\omega'\tau) + Y_{0,2}^0(\omega')\exp(2\mathrm{i}\omega'\tau) + \text{C.C.}]. \tag{37}$$

Note that in the expressions for $Y_{0,0}^0(\omega')$, $Y_{0,1}^0(\omega')$ and $Y_{0,2}^0(\omega')$, we have replaced the field parameter $r = E_c/E_a$ with a more convenient one $r = E_c^2/E^2$ and the quantity R is replaced by $\alpha = \frac{\Delta\alpha/(k_B T)}{K_0}$. With these new parameters, the limiting cases are better understood; for example $r = 0$ corresponds to pure AC field effects and $\alpha = 0$ demonstrates the properties of a non-polarizable but polar molecule. Note that both parameters are such that $0 \leqslant r \leqslant 1$ and $0 \leqslant \alpha \leqslant 1$. The Kerr function (37) presents very interesting properties. It expresses the time,

radio frequency (rf), rotator-bath parameters and more importantly the E_c/E_a dependences of the Kerr electrical birefringence (KEB). For infinitely high frequencies, the function reduces to the constant field steady state expression

$$\Phi_\infty = \frac{E_c^2}{15}\left(\left(\frac{\mu^2}{k_BT}\right)^2 + \frac{\Delta\alpha}{k_BT}\right) + \frac{E_a^2}{30}\frac{\Delta\alpha}{k_BT}. \tag{38}$$

The effect of the AC field is felt only when $\Delta\alpha = \alpha_\parallel - \alpha_\perp \neq 0$. This result is consistent with that of Doi and Edwards [21]. At very high frequencies, the AC field effects on dipole moments average out. Also, in the absence of the DC field ($r = 0$), the term $Y^0_{0,1}(\omega')$ vanishes and the result for a pure AC field is recovered.

It is important to note that, while all these results are deduced as the classical limit of a quantum theory, they recover recent results such as those of Déjardin *et al* in 1996 [24] and Hounkonnou *et al* [11] based on the Fokker–Planck equation. More recently, Déjardin *et al* [25] used the Smoluchowski equation to analyse the effect of a DC field on the relaxation time of the dynamic Kerr function. A similar procedure was adopted by Coffey *et al* [26] to tackle the same problem.

2.2. The rotating wave approximation (RWA) limit

In this limit, the solution of the rotators in the bath is assumed highly diluted, the pressure and friction are very low. The coupling parameter B or the characteristic rotator-bath frequency is very small compared with the rotator lines $\omega_l = (\overline{h}l/I)$. The dynamics of the rotator is governed mainly by free rotations and interactions with the re-orienting fields. Bath coupling affects only the frequency shifts and line widths. The absorption lines are the neat spectral lines corresponding to the different l transitions owing to non-negligible Planck constant $\overline{h}$ and finite inertia [20]. The transition frequencies are

$$\omega_{l->l\pm\Delta l} = |(E_{l\pm\Delta l} - E_l)|/\overline{h} = (2l + 1 + \Delta l)\overline{h}/2I$$

for transitions from l to $l \pm \Delta l$. At the level of linear response, $\Delta l = 1$ and $\omega_{l+1} = (l+1)\overline{h}/I$. For the lowest-order nonlinear effect (the Kerr effect to the second order in the electric field), $\Delta l = 2$ and $\omega_{2l+3} = (2l + 3)\overline{h}/I$.

The relevant dielectric matrix elements are governed by the quantum HT equations for the electrical susceptibility and the Kerr optical functions [4]:

$$\left(\frac{\partial}{\partial t} - \mathrm{i}(\omega_{l+1} + \Delta\omega_{l+1}) + \Gamma_{l+1}\right)\sigma_{l,l+1}(t) = -\mathrm{i}\frac{\mu E_a}{\overline{h}}(r + \cos\omega t)(1 - \mathrm{e}^{-\beta(E_{l+1}-E_l)}) \tag{39}$$

$$\left(\frac{\partial}{\partial t} + \gamma_l\right)\varphi_{l,l}(t) = \frac{\mu E_a}{\overline{h}}(r + \cos\omega t) \times \left(\frac{2l-1}{2l+1}\mathrm{Im}\,\sigma_{l,l+1}(t) - \mathrm{e}^{\beta(E_l-E_{l-1})}\frac{2l+3}{2l+1}\mathrm{Im}\,\sigma_{l-1,l}(t)(1-\delta_{l,0})\right) \tag{40}$$

$$\left(\frac{\partial}{\partial t} - \mathrm{i}(\omega_{2l+3} + \Delta\omega_{2l+3}\right) + \Gamma_{2l+3})\eta_{l,l+2}(t) = \mathrm{i}\frac{\mu E_a}{\overline{h}}(r + \cos\omega t)(\mathrm{e}^{-\beta(E_{l+1}-E_l)}\sigma_{l+1,l+2}(t) - \sigma_{l,l+1}(t)) - \mathrm{i}\frac{\Delta\alpha E_a^2}{2\overline{h}}(r + \cos\omega t)^2(1 - \mathrm{e}^{-\beta(E_{l+2}-E_l)}). \tag{41}$$

Here, we define the dimensionless line widths and frequency shifts:

$$\gamma_l' = \frac{I}{\overline{h}}\gamma_l = \frac{2BI}{\overline{h}}\frac{1}{2l+1}\left[l^2(1 + \frac{1}{\mathrm{e}^{\beta\overline{h}\omega_l} - 1}) + \frac{(l+1)^2}{\mathrm{e}^{\beta\overline{h}\omega_{l+1}} - 1}\right] \tag{42}$$

$$\Gamma'_{l+1} = \tfrac{1}{2}(\gamma'_l + \gamma'_{l+1}) \tag{43}$$

$$\Gamma'_{2l+3} = \tfrac{1}{2}(\gamma'_l + \gamma'_{l+2}) \tag{44}$$

$$\Delta\omega'_{l+1} = -\frac{4\overline{h}^3 B}{Ik_B^2 T^2}(2l+3) \times \sum_{n=0}^{\infty} \frac{(2n\pi)^3}{[(2n\pi)^2 + (al)^2]} \frac{1}{[(2n\pi)^2 + (a(l+1))^2][(2n\pi)^2 + (a(l+2))^2]} \tag{45}$$

and

$$\Delta\omega'_{2l+3} = -\frac{4\overline{h}^3 B}{Ik_B^2 T^2}(2l+3) \sum_{n=0}^{\infty} \frac{(2n\pi)^5 (1 + \frac{a}{(n\pi)^2}(l^2+3l+3))}{[(2n\pi)^2 + (al)^2][(2n\pi)^2 + (a(l+1))^2]} \times \frac{1}{[(2n\pi)^2 + (a(l+2))^2][(2n\pi)^2 + (a(l+3))^2]} \tag{46}$$

where $a = \overline{h}^2/Ik_BT$. These functions indicate well how line widths and frequency shifts respond to changing physical parameters like inertia, friction and temperature, and thus their utility in exploring the influence of the parameter variations on spectral lines. Note that, in our dimensionless frequency units, we define the quantum state frequency $\omega'_l = l$.

2.2.1. The electrical susceptibility. We are interested in the steady state regime. On solving equation (39) for this, we get

$$\sigma^{st}_{l,l+1}(\omega, t) = (\mu E_a/\overline{h}) \left(1 - \exp[-\frac{\overline{h}^2}{Ik_BT}(l+1)]\right) \left\{ \frac{r}{\omega_{l+1} + \Delta\omega_{l+1} + \mathrm{i}\Gamma_{l+1}} + \frac{\mathrm{e}^{\mathrm{i}\omega t}}{2(\omega_{l+1} + \Delta\omega_{l+1} - \omega + \mathrm{i}\Gamma_{l+1})} + \frac{\mathrm{e}^{-\mathrm{i}\omega t}}{2(\omega_{l+1} + \Delta\omega_{l+1} + \omega + \mathrm{i}\Gamma_{l+1})} \right\}. \tag{47}$$

The polarization is deduced as

$$P(\omega, t) = \frac{\mu^2 E_a}{3k_BT} \sum_{l=0}^{\infty} (\mathrm{e}^{-\beta E_l} - \mathrm{e}^{-\beta E_{l+1}}) \frac{l+1}{a} (l + 1 + \Delta\omega'_{l+1}) \{ r/[(l + 1 + \Delta\omega'_{l+1})^2 + \Gamma'^2_{l+1}] + ([(l + 1 + \Delta\omega'_{l+1})^2 - \omega'^2 + {\Gamma'_{l+1}}^2] \cos\omega t + 2\Gamma'_{l+1}\omega' \sin\omega t)/ ([(l + 1 + \Delta\omega'_{l+1})^2 - \omega'^2 + {\Gamma'_{l+1}}^2]^2 + 4\omega'^2 {\Gamma'_{l+1}}^2) \}. \tag{48}$$

These are the Van Vleck–Weisskopf line forms for the electrical susceptibility. Sharp separate lines result for small widths at half-heights Γ_{l+1}. For line coupling and subsequent line overlaps to be absent, thus, Γ_{l+1} should be small compared with line spacings which for the electrical susceptibility stand at $\overline{h}/I$. Note that the Boltzmann weight $\mathrm{e}^{-\beta E_l}$ appearing in the last expression renders small quantum number transitions more probable. An appropriate Taylor expansion of the Bose–Einstein factor appearing in the expression of the half-width shows that a necessary condition for dominant lines is expressed by the inequality $(B/\omega_{mean})^2 \ll a^3/4 = (\overline{h}^2/Ik_BT)^3/4$.

For $r = 0$, we define the reduced susceptibility

$$\chi_r(\omega, t) = \cos(\omega t - \alpha(\omega)) \tag{49}$$

where $\alpha(\omega)$, the phase difference between the exciting field and the induced polarization, is given by

$$\tan\alpha(\omega) = \left[\sum_{l=0}^{\infty} (\mathrm{e}^{-\beta E_l} - \mathrm{e}^{-\beta E_{l+1}})(l+1)(l + 1 + \Delta\omega'_{l+1})\Gamma'_{l+1}\omega' \right/$$

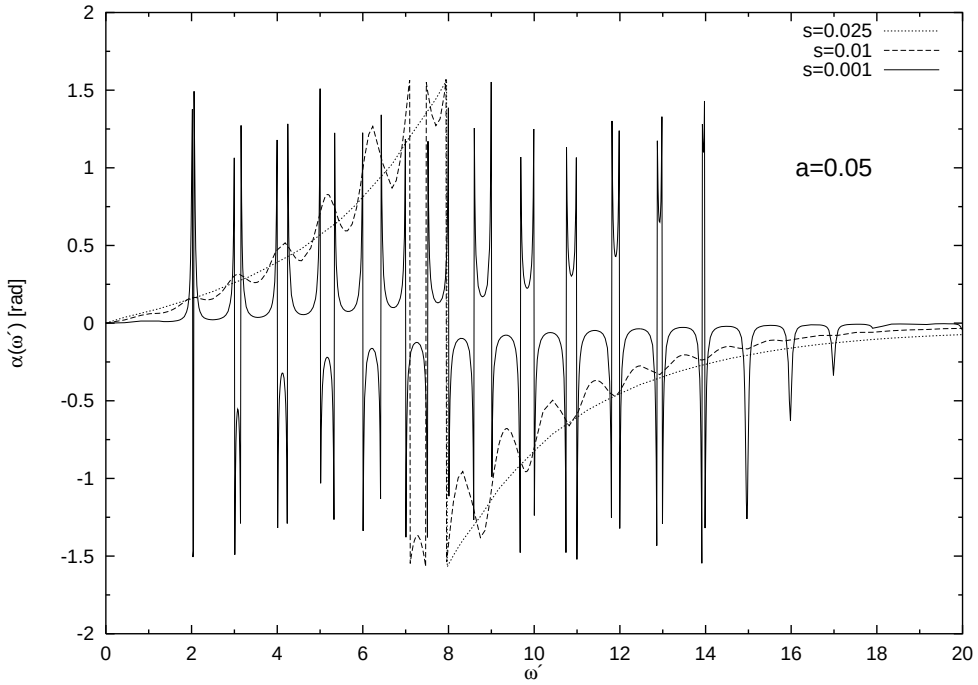

Figure 5. Plots of the phase difference $\alpha(\omega')$ (in rad) between the AC field and response function against the dimensionless frequency $\omega' = \omega/(\omega_q)$ for the ratio $a = (\omega_q/\omega_{mean})^2 = 0.05$ ($\omega_q = \overline{h}/I$) for the friction parameter $s = 1/\sqrt{\gamma} = 0.025$ ($\cdots\cdots$), $s = 0.01$ (- - - -) and $s = 0.001$ (——) (RWA).

$$\left([(l+1+\Delta\omega'_{l+1})^2 - \omega'^2 + \Gamma'^2_{l+1}]^2 + 4\omega'^2\Gamma'^2_{l+1}\right)\Bigg/$$
$$\left[\sum_{l=0}^{\infty}(\mathrm{e}^{-\beta E_l} - \mathrm{e}^{-\beta E_{l+1}})(l+1)(l+1+\Delta\omega'_{l+1})((l+1+\Delta\omega'_{l+1})^2 - \omega'^2 + \Gamma'^2_{l+1})\Bigg/\right.$$
$$\left.([(l+1+\Delta\omega'_{l+1})^2 - \omega'^2 + \Gamma'^2_{l+1}]^2 + 4\omega'^2\Gamma'^2_{l+1})\right]. \tag{50}$$

Note that for usual temperatures and simple linear molecules like HCl and DCl [22, 31], the frequency shift has a negligible contribution as it varies as $\Delta\omega'_{l+1} \sim -10^{-4}(2l+3)$ compared with the corresponding line $l+1$.

2.2.2. The Kerr function. On using the expression for $\sigma^{st}_{l,l+1}(\omega, t)$ (equation (47)) into equations (40) and (41) and solving the resulting equations for the steady state matrix elements $\varphi^{st}_{l,l}(\omega, t)$ and $\eta^{st}_{l,l+2}(\omega, t)$, we deduce that the Kerr function comprises three terms: a frequency dependent time constant term $\Phi_0(\omega)$, an ω-frequency time dependent term $\Phi_1(\omega)\mathrm{e}^{\mathrm{i}\omega t}$ and a 2ω-frequency time dependent one $\Phi_2(\omega)\mathrm{e}^{2\mathrm{i}\omega t}$ with their respective complex conjugates. In other words,

$$\Phi(\omega, t) = \Phi_0(\omega) + \Phi_1(\omega)\mathrm{e}^{\mathrm{i}\omega t} + \Phi_2(\omega)\mathrm{e}^{2\mathrm{i}\omega t} + \mathrm{C.C.} \tag{51}$$

where $\Phi_0(\omega)$, $\Phi_1(\omega)$ and $\Phi_2(\omega)$ are explicitly written out in appendix C.

Relation (51) shows how a frequency-time dependent Kerr optical function depends on field parameters like frequency and field strengths, on molecular parameters like moment of

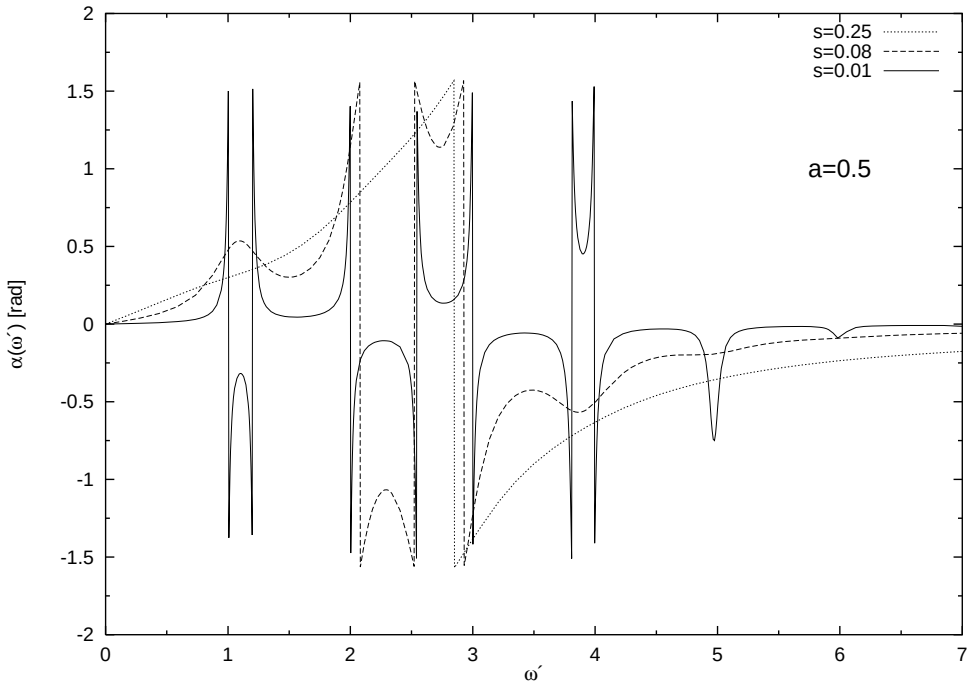

Figure 6. Plots of the phase difference $\alpha(\omega')$ (in rad) between the AC field and response function against the dimensionless frequency $\omega' = \omega/\omega_q$ for the ratio $a = (\omega_q/\omega_{mean})^2 = 0.5$ ($\omega_q = \overline{h}/I$) for the friction parameter $s = 1/\sqrt{\gamma} = 0.25$ ($\cdots\cdots$), $s = 0.08$ (- - - -) and $s = 0.01$ (——) (RWA).

inertia, dipole moment and polarizability, on bath frictional parameter and on temperature. Despite the fact that these results have been obtained in the limit of small coupling parameter B, they can still be used as a first approximation to interpret experimental results on dense bath but at very low temperatures. We point out that, unlike earlier works on electrical susceptibility which have always considered that observed spectra are mainly accounted for by transitions involving $\Delta l = \pm 1$, these results on the Kerr optical effect predict, not only $\Delta l = \pm 1$ transitions, but also those with $\Delta l = \pm 2$.

3. Discussions

(1) In constant temperature conditions, the response of a dielectric material to a low frequency external AC field is strong and is in phase with the latter for low frictional oscillator-bath and/or large inertia molecules ($\gamma = 0.5$ in figure 1). From the energetic point of view, this in-phase aspect favours the external field effect on the rotator-bath system and thus increases the system's ability to capture energy from the surroundings. On the other hand, a totally different phenomenon is observed for high frequencies where a weak response sets in, tending to annihilate the field effect by appearing in anti-phase with it (figure 2). The first convergent of the classical susceptibility function corresponding to the Rocard result (the first approximation of the inertia effect) gives a maximum phase for a frequency of $\omega = \sqrt{2}\omega_{mean}$ whatever the γ value. At this frequency value collisions result in large energy exchanges of the order of $k_B T$. For higher γ values, there is a departure from this frequency value (see figure 4).

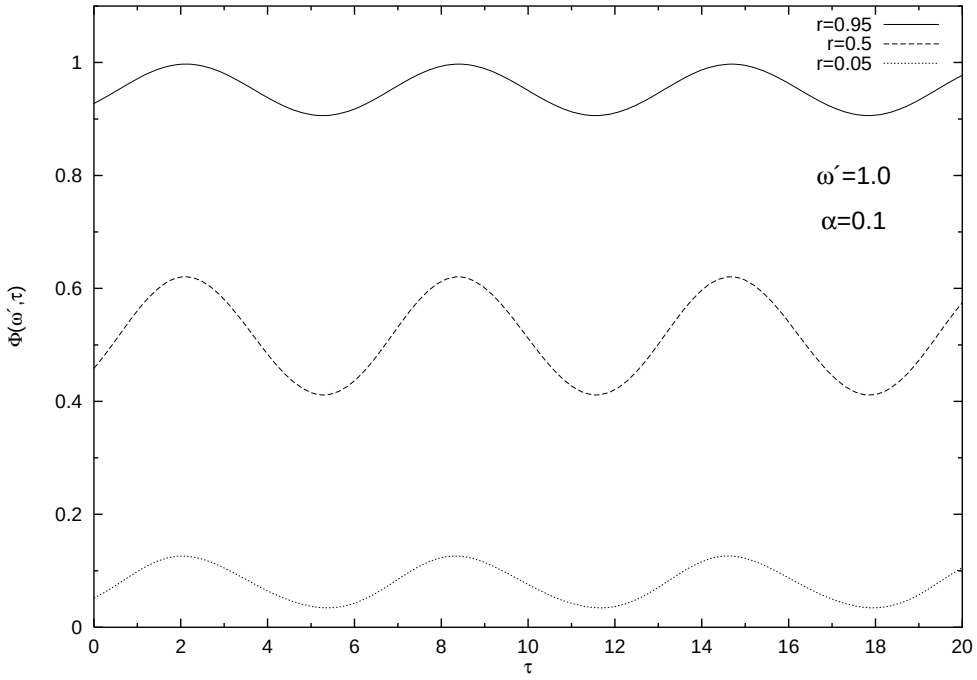

Figure 7. Plots of the classical Kerr function against the reduced time $t' = Bt$ for the field ratio $r = 0.95$ (——), $r = 0.5$ (- - - -) and $r = 0.05$ (· · · · · ·), provided $\omega/B = 1.0$ and the polarizability/dipole moment parameter $\alpha = 0.1$ ($\alpha = \Delta\alpha/k_BT/((\mu/k_BT)^2 + \Delta\alpha/k_BT)$).

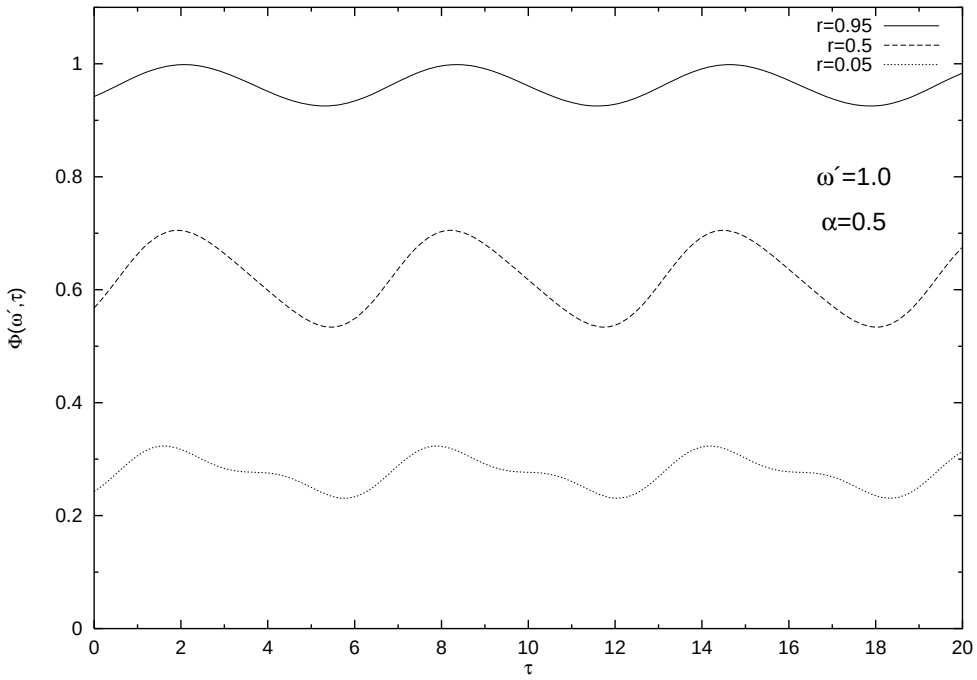

Figure 8. Plots of the classical Kerr function against the reduced time $t' = Bt$ for the field ratio $r = 0.95$ (——), $r = 0.5$ (- - - -) and $r = 0.05$ (· · · · · ·), provided $\omega/B = 1.0$ and $\alpha = 0.5$.

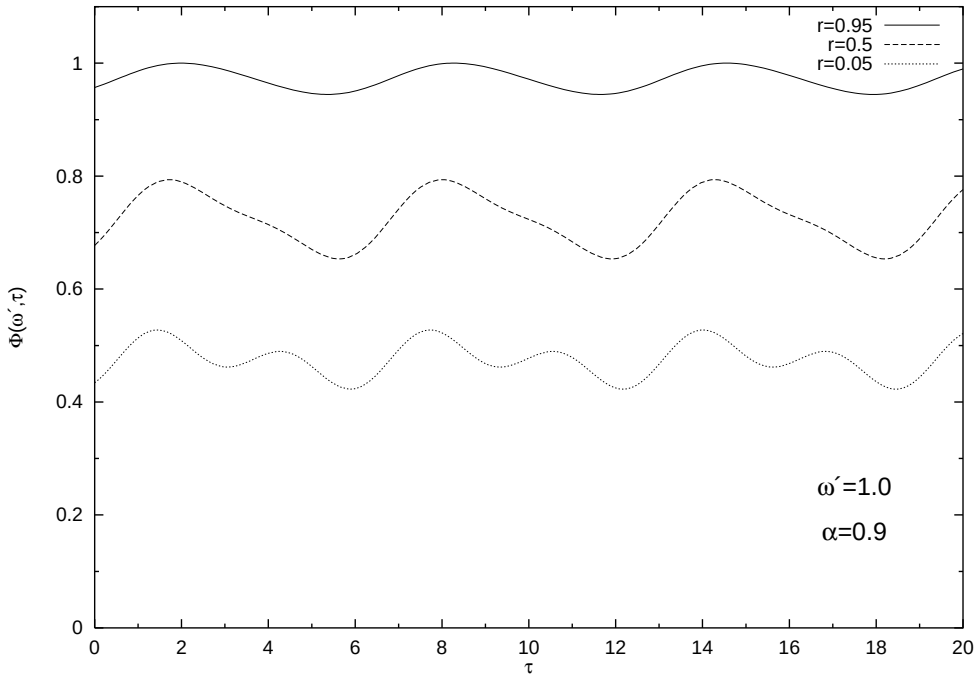

Figure 9. Plots of the classical Kerr function against the reduced time $t' = Bt$ for the field ratio $r = 0.95$ (——), $r = 0.5$ (- - - -) and $r = 0.05$ (· · · · · ·), provided $\omega/B = 1.0$ and $\alpha = 0.9$.

(2) The manifestation of quantum effects depends not only on the coupling parameter ($B = \zeta/I$) but also on the temperature–inertia parameter $a = \overline{h}^2/(Ik_BT)$. This allows us to define a necessary condition for the domination of quantum effects. The inequality

$$s = B/\omega_{mean} = 1/\sqrt{\gamma} \ll \tfrac{1}{2}(\overline{h}^2/Ik_BT)^{3/2} = a^{3/2}/2 \tag{52}$$

expresses this condition. For example, for $a = 0.05$, as the parameter s decreases from 0.025 through 0.010 to 0.001, we observe a passage from a continuous classical spectrum through broadened lines to well-defined discrete lines (figure 5); meanwhile for $a = 0.5$ quantum effects are already present even for $s = 0.08$ (see figure 6). This observation is also important for the Kerr spectra (see figure 14). In our previous paper [4], we had already remarked that, as the coupling parameter $s = B/\omega_{mean}$ decreases under fixed a, a transition from the usual continuous classical spectrum through broadened lines to separate lineforms was observed. This phenomenon was also observed experimentally by Frenkel [1] on HCl in argon while varying argon density at very low temperatures. A recent experimental study of the linear and nonlinear dielectric spectra of 4, 4′-*n*-pentyl-cyanobiphenyl (5CB) was undertaken by De Smet *et al* [27]. However, the study concerned large molecules at room temperatures. This limited the interpretation of the results in the framework of classical theories well predicted by Coffey *et al* [18] and Alexiewicz *et al* [28].

(3) The time variation of the classical Kerr electrical birefringence (KEB) is characterized by oscillations about r–ω dependent time constant values which decrease with decreasing r and with increasing frequency. The 2ω-harmonic component is dominant for small r and large α values while the single ω one dominates for intermediate and higher r values, (see figures 7–9). Physically, the doubling of period takes place by a process of progressive crushing of intermediate peak values in the KEB curve shape with increasing r. This period change is

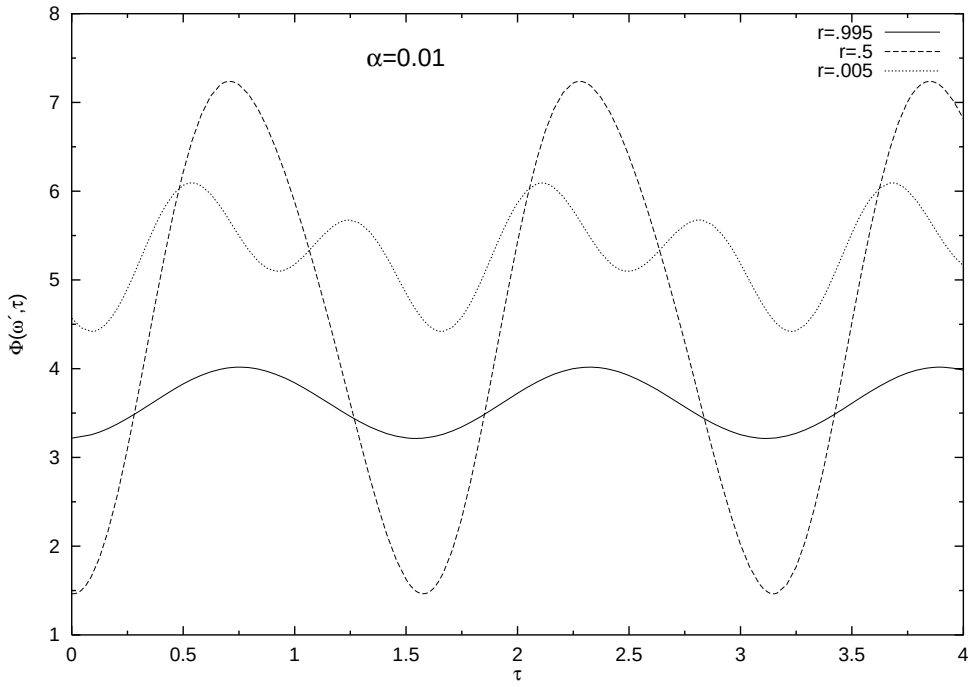

Figure 10. Plots of the quantum Kerr function $\Phi(\omega, t)$ against the dimensionless time $t' = t/(\overline{h}/I)$ for the field ratio $r = 0.95$ (——), $r = 0.5$ (- - - -) and $r = 0.05$ (· · · · · ·), provide $\omega = 4\overline{h}/I$ and $\alpha = 0.1$.

noticed by a set of pronounced transitions of non-sinusoidal periodic regimes which take place between two sinusoidal regime limits corresponding to the extreme r values ($E_a \ll E_c$ and $E_a \gg E_c$).

(4) For constant bath parameters and for small and intermediate E_c/E_a ratio, the Kerr effect increases with increasing α, presenting small amplitude distortions that disappear to form secondary peaks as α grows, portraying the progressive appearance of the influence of the 2ω-harmonic component (see figures 7–12).

(5) The Kerr spectral function for AC–DC coupling is

$$\tilde{\Phi}(\omega, \Omega) = [2\mathrm{Re}\,\Phi_0(\omega)\delta(\Omega) + \Phi_1(\omega)\delta(\Omega - \omega) + \Phi_1^*(\omega)\delta(\Omega + \omega) + \Phi_2(\omega)\delta(\Omega - 2\omega) + \Phi_2^*(\omega)\delta(\Omega + 2\omega)]. \tag{53}$$

This shows that for an AC field of given frequency, all three terms cannot be measured simultaneously. The AC–DC field coupling on dielectrics, therefore, proves to be very useful as, depending on the harmonic component observed, we are able to predict the relative strengths of permanent dipole to induced dipole effects. The 2ω-component dominates for polarizable fluids (large α) while the ω-one dominates for less polarizable fluids (small α) (see figures 7–12). More importantly, the observation of 2ω-harmonic component may also entail that the most probable rotational lines involve transitions like $l \to l \pm 2$ while the observation of ω harmonics concerns transitions $l \to l \pm 1$ (see figures 13). This last point is very important when E_c and E_a are of the same order of magnitude.

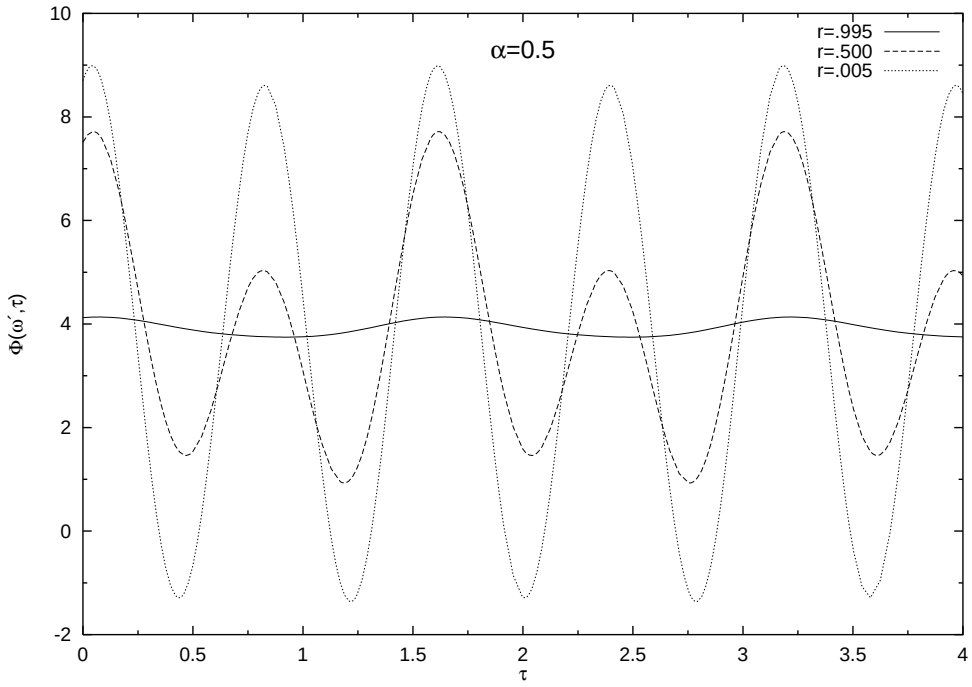

Figure 11. Plots of the quantum Kerr function $\Phi(\omega, t)$ against the dimensionless time $t' = t/(\overline{h}/I)$ for the field ratio $r = 0.995$ (——), $r = 0.5$ (- - - -) and $r = 0.05$ (· · · · · ·), provided $\omega = 4\overline{h}/I$ and $\alpha = 0.5$.

Acknowledgments

The work of JTT is financed by the Belgian Administration Générale pour la Coopération au Développement (AGCD-Belgium). The authors acknowledge the technical assistance of the Computing Center of Université Libre de Bruxelles (ULB). HMN thanks the Unité FYMA of Institut de Physique Théorique of Université Catholique de Louvain (UCL) for kind hospitality during his last three month stay in Belgium.

Appendix A. Systems of hierarchies for $Y^m_{j,l}$ and $X_{j,l}$

(Triplet 1)

$$
\begin{aligned}
&2jY^0_{j,0}(\omega') + 24b_2((j+1)Y^1_{j,0}(\omega') - jY^1_{j-1,0}(\omega')) = -2b_2S^1_{j-1}(\omega')(1-\delta_{j,0})\\
&(2j+1)Y^1_{j,0}(\omega') - \frac{b_1}{3}(Y^0_{j,0}(\omega') - Y^0_{j+1,0}(\omega')) + \frac{b_1}{3}(X_{j,0}(\omega') - X_{j+1,0}(\omega'))\\
&\qquad = -\frac{b_1}{4}[(2r^2 + 2r^2/R + 1/R)\delta_{j,0} + 2S^0_j(\omega')]\\
&[2j(2j+1)+2]X_{j,0}(\omega') - j(2j-2)X_{j-1,0}(\omega) - (j+1)(2j+2)X_{j+1,0}(\omega')\\
&\qquad -\tfrac{1}{2}Y^0_{j,0}(\omega') = \frac{b_2}{2}[-2j(j-1)S^1_{j-2}(\omega') + j(4j+5)S^1_{j-1}(\omega')\\
&\qquad -(j+1)(2j+3)S^1_j(\omega')].
\end{aligned}
\tag{54}
$$

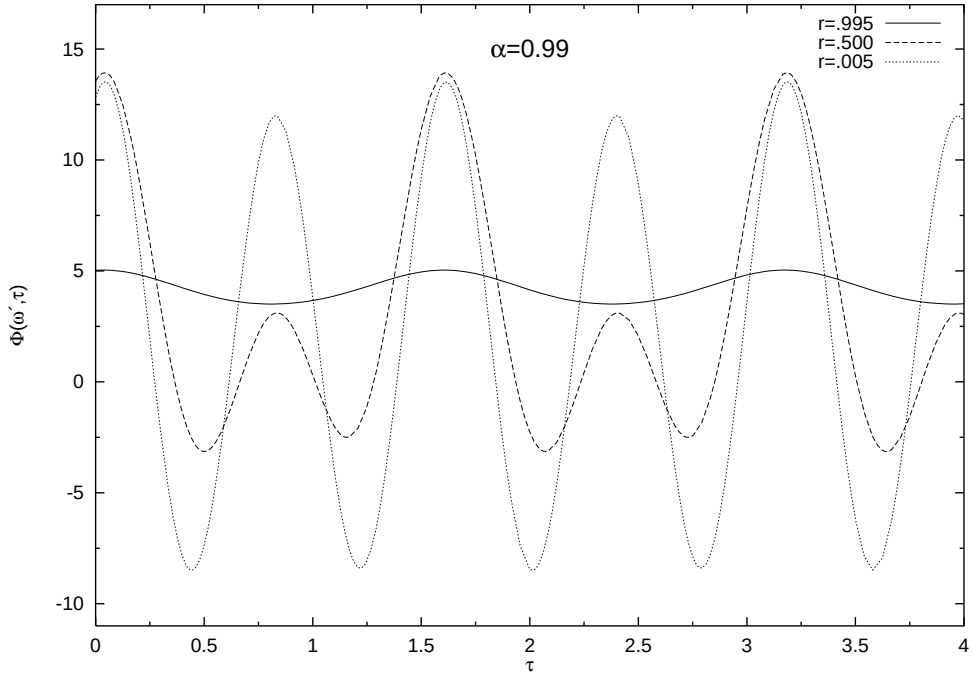

Figure 12. Plots of the quantum Kerr function $\Phi(\omega, t)$ against the dimensionless time $t' = t/(\overline{h}/I)$ for the field ratio $r = 0.995$ (——), $r = 0.5$ (- - - -) and $r = 0.05$ (· · · · · ·), provided $\omega = 4\overline{h}/I$ and $\alpha = 0.9$.

(Triplet 2)

$$
\begin{aligned}
&(\mathrm{i}\omega' + 2j)Y^0_{j,1}(\omega') + 24b_2((j+1)Y^1_{j,1}(\omega') - jY^1_{j-1,1}(\omega')) = -4rb_2S^1_{j-1}(\omega')(1-\delta_{j,0})\\
&(\mathrm{i}\omega' + 2j + 1)Y^1_{j,1}(\omega') - \frac{b_1}{3}(Y^0_{j,1}(\omega') - Y^0_{j+1,1}(\omega')) + \frac{b_1}{3}(X_{j,1}(\omega') - X_{j+1,1}(\omega'))\\
&\qquad = -r\frac{b_1}{4}[(2+4/R)\delta_{j,0} + 4S^0_j]\\
&[(2j+1)(\mathrm{i}\omega' + 2j) + 2]X_{j,1}(\omega') - j(\mathrm{i}\omega' + 2j - 2)X_{j-1,1}(\omega')\\
&\qquad -(j+1)(\mathrm{i}\omega' + 2j + 2)X_{j+1,1}(\omega') - (\tfrac{1}{2})Y^0_{j,1}(\omega')\\
&\qquad = b_2r[-2j(j-1)S^1_{j-2}(\omega')\\
&\qquad +j(4j+5)S^1_{j-1}(\omega') - (j+1)(2j+3)S^1_j(\omega')].
\end{aligned}
\tag{55}
$$

(Triplet 3)

$$
\begin{aligned}
&(2\mathrm{i}\omega' + 2j)Y^0_{j,2}(\omega') + 24b_2((j+1)Y^1_{j,2}(\omega') - jY^1_{j-1,2}(\omega')) = -2b_2S^1_{j-1}(\omega')(1-\delta_{j,0})\\
&(2\mathrm{i}\omega' + 2j + 1)Y^1_{j,2}(\omega') - \frac{b_1}{3}(Y^0_{j,2}(\omega') - Y^0_{j+1,2}(\omega')) + \frac{b_1}{3}(X_{j,2}(\omega') - X_{j+1,2}(\omega'))\\
&\qquad = -\frac{b_1}{4}\left[\frac{1}{R}\delta_{j,0} + 2S^0_j\right]\\
&[(2j+1)(2\mathrm{i}\omega' + 2j) + 2]X_{j,2}(\omega') - j(2\mathrm{i}\omega' + 2j - 2)X_{j-1,2}(\omega')\\
&\qquad -(j+1)(2\mathrm{i}\omega' + 2j + 2)X_{j+1,2}(\omega') - \tfrac{1}{2}Y^0_{j,2}(\omega')\\
&\qquad = \frac{b_2}{2}[-2j(j-1)S^1_{j-2}(\omega')\\
&\qquad +j(4j+5)S^1_{j-1}(\omega') - (j+1)(2j+3)S^1_j(\omega')]
\end{aligned}
\tag{56}
$$

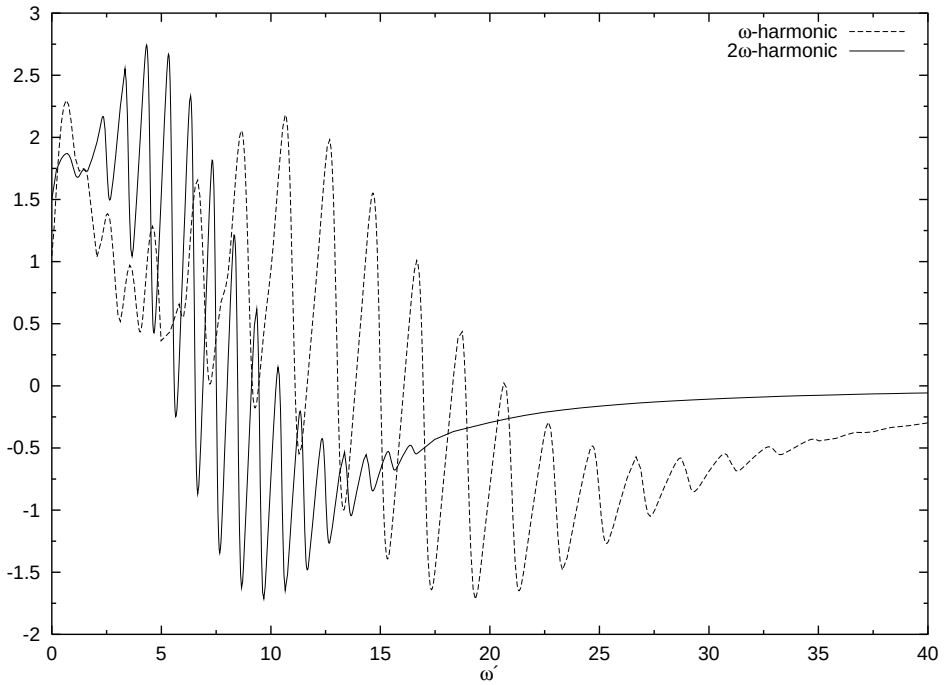

Figure 13. Plot of the real part of the ω-harmonic component (- - - -) and the 2ω-harmonic component (——) of the quantum Kerr function against the dimensionless frequency $\omega/(\overline{h}/I)$ for $a = 0.05$, $s = 0.01$, $\alpha = 0.4$ and $r = 0.5$).

where $R = \mu^2/(\Delta\alpha k_B T)$. For simplicity, we have left out the primes on each S_j^m. i denotes the complex number $\sqrt{-1}$.

Appendix B. Expressions for $Y^0_{0,0}$, $Y^0_{0,1}$ and $Y^0_{0,2}$

$$Y^0_{0,0}(\omega') = \tfrac{1}{2}(\alpha + 2r - \alpha r) + (1-\alpha)(1-r)\left\{\left(1 - \frac{\mathrm{i}\omega'}{2}\right) + \frac{2\mathrm{i}\omega'}{3(2+5\gamma)} \times\left[2 - \gamma - \cfrac{8\gamma}{2 + \mathrm{i}\omega' + \cfrac{4\gamma}{3 + \mathrm{i}\omega' + \cfrac{4\gamma}{4 + \mathrm{i}\omega' + \cdots}}} + \frac{4\gamma^2/3}{4\gamma + (2+\mathrm{i}\omega')(3 + \mathrm{i}\omega' + \cfrac{4\gamma}{4 + \mathrm{i}\omega' + \cfrac{6\gamma}{5 + \mathrm{i}\omega' + \cfrac{6\gamma}{6 + \mathrm{i}\omega' + \cdots}}})}\right]\right\} \times \frac{\gamma}{2\gamma + \mathrm{i}\omega'(1 + \mathrm{i}\omega' + \cfrac{2\gamma}{2 + \mathrm{i}\omega' + \cfrac{4\gamma}{3 + \mathrm{i}\omega' + \cfrac{4\gamma}{4 + \mathrm{i}\omega' + \cdots}}})}$$

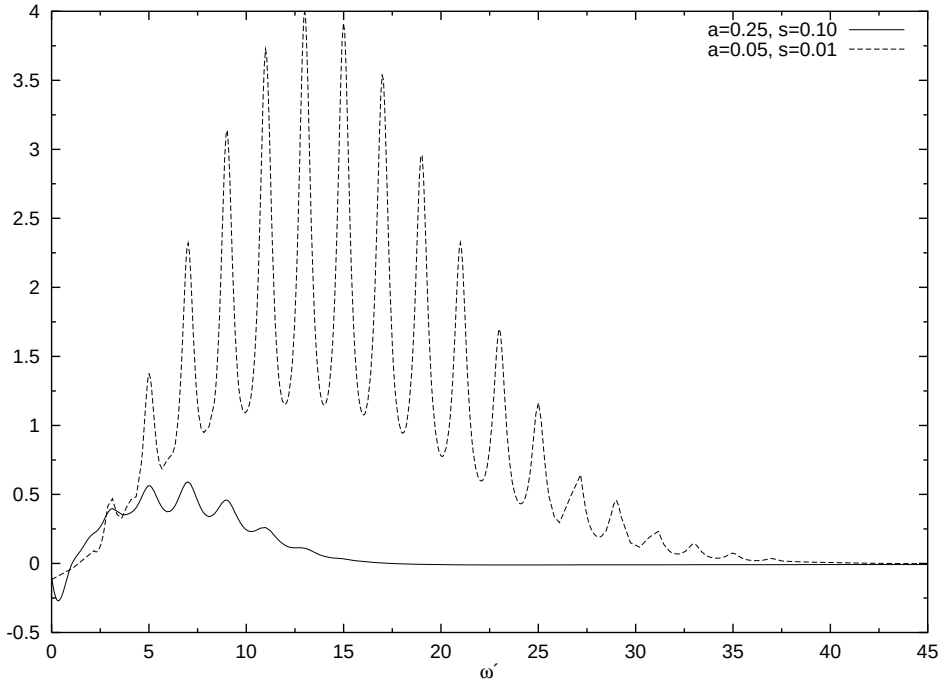

Figure 14. Plot of the imaginary part of the ω-harmonic component of the quantum Kerr function against the dimensionless frequency $\omega/(\bar{h}/I)$ for $a = 0.25$(- - - -) and $a = 0.05$(——), provided the friction parameter $s = 1/\sqrt{\gamma} = 0.01$ and the polarizability-dipole moment parameter $\alpha = 0.4$ and $r = 0.5$.

$$+\frac{64}{9}\frac{\gamma}{2+5\gamma}Y^0_{2,0}(\omega') \tag{57}$$

$$Y^0_{0,1}(\omega') = \sqrt{r(1-r)}\Bigg\{(1+2/R)\frac{6\gamma(1+\alpha)}{1+\mathrm{i}\omega'}\left(2+\mathrm{i}\omega'+4\gamma\frac{15+4\mathrm{i}\omega'}{(3+\mathrm{i}\omega')(4+\mathrm{i}\omega')}\right)$$
$$+(1-\alpha)\Bigg[\frac{24\gamma}{(1+\mathrm{i}\omega')(2+\mathrm{i}\omega')}\left(2+\mathrm{i}\omega'+4\gamma\frac{15+4\mathrm{i}\omega'}{(3+\mathrm{i}\omega')(4+\mathrm{i}\omega')}\right)$$
$$+\frac{8\mathrm{i}\omega'\gamma}{1+\mathrm{i}\omega'}-\frac{32\mathrm{i}\omega'\gamma^2}{(1+\mathrm{i}\omega')(3+\mathrm{i}\omega')(4+\mathrm{i}\omega')}\left(\frac{6(1+\mathrm{i}\omega')}{(2+\mathrm{i}\omega')}\right.$$
$$\left.-\frac{4\gamma}{4\gamma+(2+\mathrm{i}\omega')(3+\mathrm{i}\omega'+\dfrac{4\gamma}{4+\mathrm{i}\omega'+\dfrac{6\gamma}{5+\mathrm{i}\omega'+\dfrac{6\gamma}{6+\mathrm{i}\omega'+\cdots}}}}\right)\Bigg)$$
$$-\frac{192\gamma^2\mathrm{i}\omega'}{(1+\mathrm{i}\omega')(3+\mathrm{i}\omega')(2+\mathrm{i}\omega'+\dfrac{4\gamma}{3+\mathrm{i}\omega'+\dfrac{4\gamma}{4+\mathrm{i}\omega'+\dfrac{6\gamma}{5+\mathrm{i}\omega'+\cdots}}}})\Bigg]$$

$$\times\frac{\gamma}{2\gamma+\mathrm{i}\omega'(1+\mathrm{i}\omega'+\dfrac{2\gamma}{2+\mathrm{i}\omega'+\dfrac{4\gamma}{3+\mathrm{i}\omega'+\dfrac{4\gamma}{4+\mathrm{i}\omega'+\cdots}}})}$$
$$+\frac{128\gamma^2/r}{3+\mathrm{i}\omega'}Y^0_{2,1}(\omega')\Bigg\}\Bigg/\Bigg\{\left(\mathrm{i}\omega'+4\gamma\frac{3+\mathrm{i}\omega'}{(1+\mathrm{i}\omega')(2+\mathrm{i}\omega')}\right)$$
$$\times(2+\mathrm{i}\omega'+4\gamma\frac{15+4\mathrm{i}\omega'}{(3+\mathrm{i}\omega')(4+\mathrm{i}\omega')})$$
$$+\frac{8\mathrm{i}\omega'\gamma}{1+\mathrm{i}\omega'}-\frac{32\mathrm{i}\omega'\gamma^2}{(1+\mathrm{i}\omega')(2+\mathrm{i}\omega')(3+\mathrm{i}\omega')(4+\mathrm{i}\omega')}\Bigg\} \tag{58}$$

$$Y^0_{0,2}(\omega')=(1-r)\Bigg\{\frac{3\gamma\alpha}{1+2\mathrm{i}\omega'}\left(2+2\mathrm{i}\omega'+4\gamma\frac{15+8\mathrm{i}\omega'}{(3+2\mathrm{i}\omega')(4+2\mathrm{i}\omega')}\right)$$
$$+(1-\alpha)\Bigg[6\gamma\frac{2+\mathrm{i}\omega'}{(1+2\mathrm{i}\omega')(2+2\mathrm{i}\omega')}\left(2+2\mathrm{i}\omega'+4\gamma\frac{15+8\mathrm{i}\omega'}{(3+2\mathrm{i}\omega')(4+2\mathrm{i}\omega')}\right)$$
$$+\frac{8\mathrm{i}\omega'\gamma}{1+2\mathrm{i}\omega'}-\frac{96\mathrm{i}\omega'\gamma^2}{(1+2\mathrm{i}\omega')(3+2\mathrm{i}\omega')(2+\mathrm{i}\omega'+\dfrac{4\gamma}{3+\mathrm{i}\omega'+\dfrac{4\gamma}{4+\mathrm{i}\omega'+\cdots}})}\Bigg)$$
$$-16\mathrm{i}\omega'\gamma^2\frac{\left(3-\dfrac{4\gamma}{4\gamma+(2+\mathrm{i}\omega')(3+\mathrm{i}\omega'+\dfrac{4\gamma}{4+\mathrm{i}\omega'+\cdots})}+6\mathrm{i}\omega'\right)}{(1+2\mathrm{i}\omega')(2+2\mathrm{i}\omega')(3+2\mathrm{i}\omega')(4+2\mathrm{i}\omega')}\Bigg]$$
$$\times\frac{\gamma}{2\gamma+\mathrm{i}\omega'(1+\mathrm{i}\omega'+\dfrac{2\gamma}{2+\mathrm{i}\omega'+\dfrac{4\gamma}{3+\mathrm{i}\omega'+\dfrac{4\gamma}{4+\mathrm{i}\omega'+\cdots}}})}$$
$$+\frac{128\gamma^2}{(1+2\mathrm{i}\omega')(3+2\mathrm{i}\omega')}Y^0_{2,2}(\omega')\Bigg\}\Bigg/\Bigg\{\left[2\mathrm{i}\omega'+4\gamma\frac{3+4\mathrm{i}\omega'}{(1+2\mathrm{i}\omega')(2+2\mathrm{i}\omega')}\right]$$
$$\times\left[2+2\mathrm{i}\omega'+4\gamma\frac{15+8\mathrm{i}\omega'}{(3+2\mathrm{i}\omega')(4+2\mathrm{i}\omega')}\right]$$
$$+\frac{16\mathrm{i}\omega'\gamma((2+\mathrm{i}\omega')(3+\mathrm{i}\omega')(4+\mathrm{i}\omega')-4\gamma)}{(1+2\mathrm{i}\omega')(2+2\mathrm{i}\omega')(3+2\mathrm{i}\omega')(4+2\mathrm{i}\omega')}\Bigg\}. \tag{59}$$

Appendix C. The DC (Φ_0), the ω (Φ_1) and the 2ω (Φ_2) components of the quantum Kerr function

$$\Phi_0(\omega')=\frac{1}{60}E^2K_0\sum_{l=0}^{\infty}\frac{l+1}{a}\Bigg[(1-\alpha)\frac{l}{2l-1}\frac{1}{\gamma'_l}(\mathrm{e}^{-\beta E_{l-1}}-\mathrm{e}^{-\beta E_l})$$
$$\times\left(2r\frac{\Gamma'_l+\mathrm{i}(l+\Delta\omega'_l)}{(l+\Delta\omega'_l)^2+\Gamma'^2_l}+\frac{1}{2}(1-r)\frac{\Gamma'_l+\mathrm{i}(l+\Delta\omega'_l-\omega')}{(l+\Delta\omega'_l-\omega')^2+\Gamma'^2_l}\right)$$
$$-\frac{l}{2l+3}(1-\alpha)\frac{1}{\gamma'_l}(\mathrm{e}^{-\beta E_l}-\mathrm{e}^{-\beta E_{l+1}})\left(2r\frac{\Gamma'_{l+1}+\mathrm{i}(l+1+\Delta\omega'_{l+1})}{(l+1+\Delta\omega'_{l+1})^2+\Gamma'^2_{l+1}}\right.$$

$$
\begin{aligned}
&+\frac{1}{2}(1-r)\frac{\Gamma'_{l+1}+\mathrm{i}(l+1+\Delta\omega'_{l+1}-\omega')}{(l+1+\Delta\omega'_{l+1}-\omega')^2+\Gamma'^2_{l+1}}\Bigg)\\
&+\frac{3(l+2)}{2l+3}\frac{1}{(2l+3+\Delta\omega'_{2l+3})^2+\Gamma'^2_{2l+3}}\\
&\times\Bigg\{(2l+3+\Delta\omega'_{2l+3})-\mathrm{i}\Gamma'_{2l+3})\Bigg[(\mathrm{e}^{-\beta E_l}-\mathrm{e}^{-\beta E_{l+1}})\\
&\times\Bigg(2r\frac{(l+1+\Delta\omega'_{l+1}-\mathrm{i}\Gamma'_{l+1})}{(l+1+\Delta\omega'_{l+1})^2+\Gamma'^2_{l+1}}+\frac{1}{2}(1-r)\frac{(l+1+\Delta\omega'_{l+1}-\omega'-\mathrm{i}\Gamma'_{l+1})}{(l+1+\Delta\omega'_{l+1}-\omega')^2+\Gamma'^2_{l+1}}\\
&+\frac{1}{2}(1-r)\frac{(l+1+\Delta\omega'_{l+1}+\omega'-\mathrm{i}\Gamma'_{l+1})}{(l+1+\Delta\omega'_{l+1}+\omega')^2+\Gamma'^2_{l+1}}\Bigg)-(\mathrm{e}^{-\beta E_{l+1}}-\mathrm{e}^{-\beta E_{l+2}})\\
&\times\Bigg(2r\frac{(l+2+\Delta\omega'_{l+2}-\mathrm{i}\Gamma'_{l+2})}{(l+2+\Delta\omega'_{l+2})^2+\Gamma'^2_{l+2}}+\frac{1}{2}(1-r)\frac{(l+2+\Delta\omega'_{l+2}-\omega'-\mathrm{i}\Gamma'_{l+2})}{(l+2+\Delta\omega'_{l+2}-\omega')^2+\Gamma'^2_{l+2}}\\
&+\frac{1}{2}(1-r)\frac{(l+2+\Delta\omega'_{l+2}+\omega'-\mathrm{i}\Gamma'_{l+2})}{(l+2l+\Delta\omega'_{l+2}+\omega')^2+\Gamma'^2_{l+2}}\Bigg)\Bigg](1-\alpha)\\
&+\frac{\alpha}{2}(\mathrm{e}^{-\beta E_l}-\mathrm{e}^{-\beta E_{l+2}})(2l+3+\Delta\omega'_{2l+3})\Bigg\}\Bigg]
\end{aligned}
\tag{60}
$$

$$
\begin{aligned}
\Phi_1(\omega')=\frac{\sqrt{r(1-r)}}{60}E^2K_0\sum_{l=0}^{\infty}\frac{l+1}{a}\Bigg[&\frac{2(1-\alpha)(\gamma'_l-\mathrm{i}\omega')}{\gamma'^2_l+\omega'^2}\Bigg\{\frac{l}{2l+3}(\mathrm{e}^{-\beta E_l}-\mathrm{e}^{-\beta E_{l+1}})\\
&\times\Bigg(\frac{\Gamma'_{l+1}}{(l+1+\Delta\omega'_{l+1})^2+\Gamma'^2_{l+1}}+\frac{\Gamma'_{l+1}+\mathrm{i}(l+1+\Delta\omega'_{l+1}+\omega')}{(l+1+\Delta\omega'_{l+1}+\omega')^2+\Gamma'^2_{l+1}}\\
&-\frac{\Gamma'_{l+1}+\mathrm{i}(l+1+\Delta\omega'_{l+1}-\omega')}{(l+1+\Delta\omega'_{l+1}-\omega')^2+\Gamma'^2_{l+1}}\Bigg)-\frac{l}{2l-1}(\mathrm{e}^{-\beta E_{l-1}}-\mathrm{e}^{-\beta E_l})\\
&\times\Bigg(\frac{\Gamma'_l}{(l+\Delta\omega'_l)^2+\Gamma'^2_l}+\frac{\Gamma'_l+\mathrm{i}(l+\Delta\omega'_l+\omega')}{(l+\Delta\omega'_l+\omega')^2+\Gamma'^2_l}\\
&-\frac{\Gamma'_l+\mathrm{i}(l+\Delta\omega'_l-\omega')}{(l+\Delta\omega'_l-\omega')^2+\Gamma'^2_l}\Bigg)\Bigg\}+\frac{3(l+2)}{2l+3}\\
&\times\frac{(2l+3+\Delta\omega'_{2l+3})^2-\omega'^2-2\mathrm{i}\omega'\Gamma'_{2l+3}}{[(2l+3+\Delta\omega'_{2l+3})^2-\omega'^2+\Gamma'^2_{2l+3}]^2+4\omega'^2\Gamma'^2_{2l+3}}\Bigg\{(1-\alpha)(2l+3+\Delta\omega'_{2l+3}\\
&+\omega'-\mathrm{i}\Gamma'_{2l+3})\Bigg[(\mathrm{e}^{-\beta E_l}-\mathrm{e}^{-\beta E_{l+1}})\Bigg(\frac{l+1+\Delta\omega'_{l+1}-\omega'-\mathrm{i}\Gamma'_{l+1}}{(l+1+\Delta\omega'_{l+1}-\omega')^2+\Gamma'^2_{l+1}}\\
&+\frac{l+1+\Delta\omega'_{l+1}-\mathrm{i}\Gamma'_{l+1}-}{(l+1+\Delta\omega'_{l+1})^2+\Gamma'^2_{l+1}}\Bigg)-(\mathrm{e}^{-\beta E_{l+1}}-\mathrm{e}^{-\beta E_{l+2}})\\
&\times\Bigg(\frac{(l+2+\Delta\omega'_{l+2}-\omega'-\mathrm{i}\Gamma'_{l+2})}{(l+2+\Delta\omega'_{l+2}-\omega')^2+\Gamma'^2_{l+2}}+\frac{l+2+\Delta\omega'_{l+2}-\mathrm{i}\Gamma'_{l+2}}{(l+2+\Delta\omega'_{l+2})^2+\Gamma'^2_{l+2}}\Bigg)\Bigg]\\
&+(2l+3+\Delta\omega'_{2l+3}-\omega'+\mathrm{i}\Gamma'_{2l+3})\Bigg[(\mathrm{e}^{-\beta E_l}-\mathrm{e}^{-\beta E_{l+1}})\\
&\times\Bigg(\frac{l+1+\Delta\omega'_{l+1}+\omega'+\mathrm{i}\Gamma'_{l+1}}{(l+1+\Delta\omega'_{l+1}-\omega')^2+\Gamma'^2_{l+1}}+\frac{l+1+\Delta\omega'_{l+1}+\mathrm{i}\Gamma'_{l+1}}{(l+1+\Delta\omega'_{l+1})^2+\Gamma'^2_{l+1}}\Bigg)\\
&-(\mathrm{e}^{-\beta E_{l+1}}-\mathrm{e}^{-\beta E_{l+2}})\Bigg(\frac{l+2+\Delta\omega'_{l+2}+\omega'+\mathrm{i}\Gamma'_{l+2}}{(l+2+\Delta\omega'_{l+2}-\omega')^2+\Gamma'^2_{l+2}}
\end{aligned}
$$

$$+\frac{l+2+\Delta\omega'_{l+2}+\mathrm{i}\Gamma'_{l+2}}{(l+2+\Delta\omega'_{l+2})^2+\Gamma'^2_{l+2}}\Bigg)\Bigg](1-\alpha)+\alpha(2l+3+\Delta\omega'_{2l+3})$$
$$\times(\mathrm{e}^{-\beta E_l}-\mathrm{e}^{-\beta E_{l+2}})\Bigg\}\Bigg] \tag{61}$$

$$\Phi_2(\omega')=\frac{(1-r)}{60}E^2K_0\sum_{l=0}^{\infty}\frac{l+1}{a}\Bigg[\frac{2(1-\alpha)(\gamma'_l-2\mathrm{i}\omega')}{\gamma'^2_l+4\omega'^2}\Bigg\{\frac{l}{2l+3}(\mathrm{e}^{-\beta E_l}-\mathrm{e}^{-\beta E_{l+1}})$$
$$\times\Bigg(\frac{\Gamma'_{l+1}+\mathrm{i}(l+1+\Delta\omega'_{l+1}+\omega')}{(l+1+\Delta\omega'_{l+1}+\omega')^2+\Gamma'^2_{l+1}}-\frac{\Gamma'_{l+1}+\mathrm{i}(l+1+\Delta\omega'_{l+1}-\omega')}{(l+1+\Delta\omega'_{l+1}-\omega')^2+\Gamma'^2_{l+1}}\Bigg)$$
$$-\frac{l}{2l-1}(\mathrm{e}^{-\beta E_{l-1}}-\mathrm{e}^{-\beta E_l})\Bigg[\frac{(\Gamma'_l+\mathrm{i}(l+\Delta\omega'_l+\omega')}{(l+\Delta\omega'_l+\omega')^2+\Gamma'^2_l}-$$
$$-\frac{\Gamma'_l+\mathrm{i}(l+\Delta\omega'_l-\omega')}{(l+\Delta\omega'_l-\omega')^2+\Gamma'^2_l}\Bigg]\Bigg\}+\frac{3(l+2)}{2l+3}$$
$$\times\Big(\frac{2l+3+\Delta\omega'_{2l+3})^2-4\omega'^2-4\mathrm{i}\omega'\Gamma'_{2l+3}}{[(2l+3+\Delta\omega'_{2l+3})^2-4\omega'^2+\Gamma'^2_{2l+3}]^2+16\omega'^2\Gamma'^2_{2l+3}}\Bigg\}(2l+3+\Delta\omega'_{2l+3}$$
$$+2\omega'-\mathrm{i}\Gamma'_{2l+3})\Bigg((\mathrm{e}^{-\beta E_l}-\mathrm{e}^{-\beta E_{l+1}})\frac{l+1+\Delta\omega'_{l+1}-\omega'-\mathrm{i}\Gamma'_{l+1}}{(l+1+\Delta\omega'_{l+1}-\omega')^2+\Gamma'^2_{l+1}}$$
$$-(\mathrm{e}^{-\beta E_{l+1}}-\mathrm{e}^{-\beta E_{l+2}})\frac{(l+2+\Delta\omega'_{l+2}+\omega'-\mathrm{i}\Gamma'_{l+2})}{(l+2+\Delta\omega'_{l+2}+\omega')^2+\Gamma'^2_{l+2}}\Bigg)(1-\alpha)$$
$$+(2l+3+\Delta\omega'_{2l+3}-2\omega'+\mathrm{i}\Gamma'_{2l+3})\Bigg((\mathrm{e}^{-\beta E_l}-\mathrm{e}^{-\beta E_{l+1}})$$
$$\times\frac{l+1+\Delta\omega'_{l+1}+\omega'+\mathrm{i}\Gamma'_{l+1})}{(l+1+\Delta\omega'_{l+1}+\omega')^2+\Gamma'^2_{l+1}}-(\mathrm{e}^{-\beta E_{l+1}}-\mathrm{e}^{-\beta E_{l+2}})$$
$$\times\frac{l+2+\Delta\omega'_{l+2}+\omega'+\mathrm{i}\Gamma'_{l+2}}{(l+2+\Delta\omega'_{l+2}-\omega')^2+\Gamma'^2_{l+2}}\Bigg)(1-\alpha)$$
$$+\alpha(2l+3+\Delta\omega'_{2l+3})(\mathrm{e}^{-\beta E_l}-\mathrm{e}^{-\beta E_{l+2}})\Bigg\}\Bigg]. \tag{62}$$

References

[1] Frenkel D 1977 Rotational relaxation of linear rigid molecules in dense noble gases *Thesis of Doctorat ès Sciences* Universiteit van Amsterdam, Netherlands
[2] Navez P and Hounkonnou M N 1995 *J. Phys. A: Math. Gen.* **28** 6345
[3] Titantah J T and Hounkonnou M N 1997 *J. Phys. A: Math. Gen.* **30** 6327
[4] Titantah J T and Hounkonnou M N 1997 *J. Phys. A: Math. Gen.* **30** 6347
[5] Morita A 1978 *J. Phys. D: Appl. Phys.* **11** L9 4708
[6] Morita A and Watanabe H 1979 *J. Chem. Phys.* **70** 4708
[7] Matsumoto M, Watanabe H and Yoshioka K 1970 *J. Phys. Chem.* **74** 2182
[8] Coffey W T 1990 *J. Chem. Phys.* **93** 724
[9] Coffey W T 1991 *J. Chem. Phys.* **95** 2026
[10] Morita A 1982 *J. Chem. Phys.* **76** 3198
[11] Hounkonnou M N, Ronveaux A and Navez P 1994 *J. Phys. A: Math. Gen.* **27** 6635
[12] Navez P and Hounkonnou M N 1994 *J. Phys. A: Math. Gen.* **27** 6657
[13] Hounkonnou M N, Ronveaux A and Hazoumé R P 1991 *Physica* **179** 569
[14] Hounkonnou M N 1991 *J. Chem. Soc. Faraday Trans.* **87** 297
[15] Hounkonnou M N and Ronveaux A 1992 *Acta. Phys.* **82** 425
[16] Filippini J C 1972 *PhD Thesis* Université de Grenoble, France
[17] Navez P 1995 *Thèse de Doctorat ès Sciences* Université Catholique de Louvain, Belgium

[18] Coffey W T and Paranjape B V 1978 *Proc. R. Ir. Acad.* **78** 17
[19] Morita A and Watanabe H 1987 *Phys. Rev.* **35** 2690
[20] Gross E P 1955 *J. Chem. Phys.* **23** 1415
[21] Doi M and Edwards S F 1986 *The Theory of Polymer Dynamics* (Oxford: Clarendon)
[22] Morita A, Walker S and Calderwood J H 1976 *J. Phys. D: Appl. Phys.* **9** 2485
[23] Sack R A 1957 *Proc. Phys. Soc.* B **70** 402–13
Sack R A 1957 *Proc. Phys. Soc.* B **70** 414–26
[24] Déjardin J L, Déjardin P M and Kalmykov Yu P 1996 *J. Chem. Phys.* **106** 5824
[25] Déjardin J L, Déjardin P M and Kalmykov Yu P 1997 *J. Chem. Phys.* **107** 508
[26] Coffey W T, Déjardin J L and Kalmykov Yu P 1996 *Phys. Rev.* E **54** 6462
[27] De Smet K, Hellemans L, Rouleau J F and Bose T K 1998 *Phys. Rev.* E **57** 1384
[28] Alexiewicz W and Kasprvicz-Kielich B 1993 *Modern Nonlinear Optics Part I* vol 85, ed M Evans and S Kielich (New York: Wiley)
[29] McConnel J 1980 *Rotational Brownian Motion and Dielectric Theory* (New York: Academic)
[30] Lindenberg k and West B J 1991 *The Non Equilibrium Statistical Mechanics of Open and Closed Systems* (New York: VCH)
[31] Stark B 1967 *Atomic and Molecular Constants from Microscopic Spectroscopy* (Berlin: Springer)